

# Efficient Discovery of Heterogeneous Treatment Effects in Randomized Experiments via Anomalous Pattern Detection

**Edward McFowland III**

Information and Decision Sciences,  
Carlson School of Management,  
University of Minnesota

**Sriram Somanchi**

IT, Analytics, and Operations,  
Mendoza College of Business,  
University of Notre Dame

**Daniel B. Neill**

Event and Pattern Detection Laboratory,  
H.J. Heinz III College,  
Carnegie Mellon University

## Abstract

The randomized experiment is an important tool for inferring the causal impact of an intervention. The most common analysis conducted in this context is the estimation of the average treatment effect (ATE). However, the recent literature on heterogeneous treatment effects demonstrates the utility of estimating the marginal conditional average treatment effect (MCATE), i.e., the average treatment effect for a subpopulation of respondents who share a particular subset of covariates. Additionally, the literature proposes the use of statistical learning methods to estimate the exponential number of MCATEs that exist in the data. However, each proposed method makes its own set of restrictive assumptions about the intervention's effects, the underlying data generating processes, and which subpopulations (MCATEs) to explicitly estimate. Moreover, the majority of the literature provides no mechanism to identify which subpopulations are the most affected—beyond manual inspection—and provides little guarantee on the correctness of the identified subpopulations. Therefore, we propose Treatment Effect Subset Scan (TESS), a new method for discovering which subpopulation in a randomized experiment is most significantly affected by a treatment. We frame this challenge as a pattern detection problem where we maximize a nonparametric scan statistic (measurement of distributional divergence) over subpopulations, while being parsimonious in which specific subpopulations to evaluate. Furthermore, we identify the subpopulation which experiences the largest distributional change as a result of the intervention, while making minimal assumptions about the intervention's effects or the underlying data generating process. In addition to the algorithm, we demonstrate that the asymptotic Type I and II error can be controlled, and provide sufficient conditions for detection consistency—i.e., exact identification of the affected subpopulation. Finally, we validate the efficacy of the method by discovering heterogeneous treatment effects in simulations and in real-world data from a well-known program evaluation study.

*Keywords:* causal inference, program evaluation, algorithms, distributional average treatment effect, treatment effect subset scan

# 1 Introduction

The randomized experiment is employed across many empirical scientific disciplines, most prevalently in the biomedical and social sciences, as an important tool for scientific discovery, by estimating the causal impact of a particular stimulus, treatment or intervention. Traditionally, randomized experiments involved small numbers of records, outcomes, and covariates, as there were many challenges to both conducting and analyzing large-scale experiments. However, we now live in a world awash with large quantities of fine-grained data, and there is a growing interest in, and ability to conduct, large experiments. In political science, large-scale field experiments are used to study how subjects will respond to campaign outreach, to improve campaign efficiency and donations, and to gauge voter preferences and campaign persuasiveness [30]. In development and behavioral economics, catalyzed by organizations like the Abdul Latif Jameel Poverty Action Lab, large-scale experiments are being conducted to inform policy in areas including poverty, education, health, microfinance, and governance [12]. In the natural sciences and bioinformatics, experiments now include large quantities of genetic information, enabling personalized medicine and the data-driven discovery of new biological phenomena [1, 2]. Finally, web-facing organizations—e.g., Google, Microsoft, Amazon, Facebook, and eBay—conduct hundreds of large-scale online experiments daily to measure advertisement effectiveness, guide product development, expedite service adoption, and understand user behaviors [25]. However, the growth in size of data has not necessarily borne out concurrent growth in knowledge about the processes being studied. Although the challenges for running large-scale experiments have largely been overcome, attempts to analyze these experiments to their fullest and gain actionable insights about how different subpopulations have been affected by treatment are seemingly still nascent, suggesting an unmet need for scalable tools to support both efficient search and statistical veracity of the discoveries.

The increasing popularity of large-scale experiments has resulted in a widespread interest in discovering more fine-grained truths about experimental units, most prominently in the form of heterogeneous treatment effects. In most experiments, the estimate of interest is the average effect of the treatment of the sampled population. However, this population is typically diverse and therefore may experience widely varying responses to an intervention. A portion of this variability may result from systematic differences in the population, potentially captured in the observed covariates. Each combination of covariate values defines a characteristic profile, and picks out a subpopulation—e.g., the simple profile gender = “male” or the more specific profile gender = “female” & race = “A”. There are exponentially many such subpopulations—with respect to the number of observable covariates—which can lead to poor estimation of their various treatment effects in smaller scale experiments. Additionally, there is the challenge of overcoming multiple hypothesis testing and a question of unprincipled post-hoc investigation, searching for a fortuitously statistically significant result [6, 41]. These valid concerns with the traditional approach to identifying affected subpopulations serve as an impetus for the development of new methods, because uncovering affected subpopulations can lead to important scientific progress. For example, the FDA’s approval of the first race-specific drug BiDil—whose original pattern of significantly improved outcomes for African-American subjects was discovered during a post-hoc analysis of two previous and more general randomized experiments [10, 11]—is considered by the FDA as a promising step toward personalized medicine [15]. Conversely, failing to uncover affected subpopulations or to disentangle the subpopulation that is truly driving a more general effect can have non-trivial consequences. This can be particularly troublesome in the reality of public policy, when such conclusions drive the implementation of large and costly social programs because of their perceived benefits. For example, the Perry preschool project, a well studied and cited 1962 randomized experiment, finds extremely significant educational and life outcomes for early-intervention (pre-school) education [4, 8, 32]. However, a re-analysis of the data focused on treatment effect heterogeneity and multiple hypothesis testing [3] concludes that only girls experience substantial benefits, while the intervention had a non-significant impact on boys. The results from the Perry preschool were fundamental to the creation of the Head Start pre-school program [4] a national social program of the United States Department of Health and Human Services that provides, among other services, early childhood education to low-income children. If large-scale policy decisions are made as a result of such experiments, then it is clear that identifying whether there is heterogeneity in treatment effects should be an integral component of the analysis.

The emergence of large-scale experiments in the social sciences, the growing interest in heterogeneous treatment effects, and the need to address unprincipled post-hoc investigation, present a new set of analytical challenges that traditional social science methods are inadequately constructed to handle [39]: *estimating* the regularities and patterns in data at a large scale, in addition to *discovering* (subtle) novel patterns that are potentially relevant, is both computationally demanding and statistically precarious. As a result, there is an increasing, vibrant literature where statistical learning techniques are used to address the challenge of estimating heterogeneous treatment effects in large-scale randomized experiments, replacing post-hoc searching with a data-driven method for investigation and discovery (§2). However, these methods exclusively estimate treatment effects as mean shifts in the outcomes of interest, rather than more subtle changes in the outcome distribution, and provide little focus on the challenge of discovering which subpopulation in the experiment exhibits the *most significant* treatment effects.

In this work, we propose a new framework—Treatment Effect Subset Scanning (TESS)—for *discovering* which subpopulations in a randomized experiment are most significantly affected by a treatment. TESS frames the challenge of identifying the affected subpopulation as a problem of *anomalous pattern detection*, with the goal of maximizing detection power for subtle, nuanced, and heterogeneous treatment effects. Previous work in anomalous pattern detection [28] identifies subsets of data records for which some subset of attributes is generated by an (unknown) anomalous process rather than the background process which generated the remaining data. In our context—identifying subpopulations affected by treatment—the background process is the data generating process of the control group, which therefore provides an expectation for the outcome distribution under the null hypothesis of no treatment effect. Treatment subpopulations, self-similar groups of treatment units affected similarly by the treatment, will have observed outcome distributions that are unexpected given the distributions estimated from their corresponding control groups. We then scan over subpopulations to identify which subpopulation experiences the largest change in its outcome distribution, as measured by distributional goodness-of-fit statistics, as a result of the treatment. This approach makes minimal assumptions about the intervention’s effects or the underlying data generating process.

The remainder of this work begins with a review of recent statistical learning methods to estimate heterogeneous treatment effects (HTE), and an outline of general gaps that exist in the literature (Section 2). In Section 3, we propose a new class of causal estimands which generalizes the common HTE estimands and helps to address their limitations. Section 4 presents our computationally efficient TESS algorithm, which can identify the subpopulation that experiences the largest distributional change as a result of the treatment while disregarding provably sub-optimal subpopulations. Additionally, we demonstrate that the probability of committing Type I and II errors can be bounded asymptotically and we provide sufficient conditions under which our framework will discover the exact subpopulation of interest (§4.5). In Section 5 we demonstrate empirically that our framework exhibits significantly more power to detect subtle signals than current methods, while also providing more precise characterization of the affected subpopulation. We then use TESS to conduct an exploratory analysis of the well-known Tennessee STAR [42] study, discovering previously unidentified treatment effect heterogeneity. Section 6 concludes the paper.

## 2 Related Work

Heterogeneity in treatment effects is studied across many disciplines. In medicine and biostatistics, identification of heterogeneity is described as “subgroup analysis”; this is traditionally regarded as a form of post-hoc analysis and discouraged unless subgroups are pre-planned and specified before data acquisition [6, 24, 27, 41]. In psychology, the term “moderator” is used to describe a variable that affects the relationship (magnitude, direction, or both) between an independent and dependent variable: the moderator can be thought of as the dimension along which the treatment may have a differing effect. In economics and public policy, measuring treatment effects is often described as program evaluation, as the treatment of interest is typically the implementation of a social program and the quantity of interest is related to improving social welfare. Program evaluation is typically focused on mechanisms that allow the substantiation of causal claims in non-randomized studies [22]. In most of the above disciplines, the typical approach to effect identification is to specify a model of the relationship between variables (usually, linear regression) based

on theory or intuition, estimate parameters of the model from data, and test the statistical significance of these parameters. When there is interest in identifying treatment heterogeneity, the researcher is expected to pre-specify the model with the form of heterogeneity included. In the absence of sufficient prior knowledge to guide the precise model specification, it is common to attempt multiple specifications and tests, which can quickly devolve into an unprincipled search. In response, some medical and social science disciplines require pre-analysis plans, which can impede the knowledge discovery process. We argue that these challenges necessitate new data-driven tools that enable the *discovery* of unknown, and possibly subtle, treatment effects on subpopulations, while avoiding the pitfalls created by multiple testing and post-hoc analysis.

There has been a growing literature using statistical learning methods to provide data-driven approaches for estimating heterogeneous treatment effects in randomized experiments, including both sparse (regularized) regression models and tree-based methods. Popular penalized regression models include the LASSO [36] and ridge regression [20]. Recent work has adapted regularization to the causal setting and specifically to treatment effect heterogeneity [21, 35, 41], proposing methods that frame the treatment effect estimation problem as one of L1-regularized (LASSO) model selection. Although these regularized regression methods select and estimate the importance of covariates, they are still subject to the possibly restrictive assumptions and limitations of (linear) regression, including requiring the researcher to specify which covariate and treatment interactions to include, compromising their ability to *discover* unexpected treatment patterns in subpopulations.

Several other methods [7, 34] select subpopulations and estimate treatment effects using the well-known regression tree, which recursively partitions the data into homogeneous subpopulations that share a subset of covariate profile values and have similar outcomes. Although a regression tree can adaptively approximate even complex functions, its effectiveness can be severely compromised in many settings as a result of its greedy partitioning: tree models can be unstable; they can provide extremely discontinuous approximations of an underlying smooth function, limiting overall accuracy; and they can struggle to estimate functions which exhibit specific properties, including when a small proportion of the covariates constitute the influential interactions [16]. The “Causal Tree” approach of [7] provides new cross-validation criteria that allow a predictive tree to directly estimate a treatment effect, accounting for the biases resulting from selection of partitions. However, the proposed method is still subject to the limitations of a tree-based model.

Subsequent improvements on the single tree model [18, 19, 40] propose the use of ensemble methods for treatment effect estimation. [18] propose the use of Bayesian Additive Regression Trees and [40] propose the use of Random Forests, both of which improve upon the single regression tree by combining the predictions of a collection of trees. [19] observes that each of the machine learning methods proposed for model selection make “necessary and consequential” (implicit) assumptions in their modeling procedure, whose validity will vary given the specific problem context. Therefore, the authors propose a general ensemble method that brings together various models, where the weights of their estimates are learned from cross-validation. Combining the predictions of multiple models provide more stable and smooth function estimates [40]; however, they lose the interpretability of natural groupings (e.g., specific combinations of covariates or clearly defined leaves) which is important for identifying affected subpopulations.

## 2.1 Addressing limitations of the prior literature

Our proposed methodology for Treatment Effect Subset Scanning (TESS) differs substantially from the prior literature in two main aspects: identifying **general changes in distribution** rather than mean shifts, and a focus on **detecting the subpopulations most significantly affected by treatment** rather than estimating treatment effects for all individuals. First, the stated objective of the majority of methods in the current literature is estimating the average treatment effect (ATE), for the population or some subpopulations. The ATE measures the difference between the means of the treatment and control outcome distributions but cannot identify other changes in distribution. Anscombe’s quartet [5] is a classic example of datasets which have very different distributions but identical first and second moments. In such cases, the ATE will fail to identify an effect, leading to incorrect assumptions about the similarity of the distributions. In other cases, a treatment (such as a policy change which impacts only the very rich or the very poor) may substantially affect various quantile values of the distribution with only slight shifts in the mean. In such

cases, estimating the ATE would have low power to identify these distributional changes.

Second, the prior literature on heterogeneous treatment effects is primarily focused on estimating the treatment effect for each individual or for a small set of manually defined subpopulations (e.g., estimating separate effects for males vs. females). To the best of our knowledge, none of these approaches provide a mechanism to automatically detect which subpopulations exhibit the most significant treatment effects. Our TESS framework is explicitly designed for subpopulation discovery, with the twin goals of *maximizing detection power*, the ability to distinguish between experiments with a subtle heterogeneous treatment effect and those with no treatment effect, and *detection accuracy*, the ability to precisely identify the affected subpopulation. This allows us to provide theoretical guarantees on the results of discovery as well as improving both detection power and accuracy in practice.

In contrast, the prior literature can be roughly divided into three groups. Methods such as [40] produce separate estimates of the treatment effect for each individual (or set of individuals who are identical on all observed covariates). While such methods can produce a list of treated individuals ranked by estimated treatment effects, this provides little continuity across individuals, with no principled way to identify affected subpopulations or to distinguish significant heterogeneous treatment effects from noise. Manually grouping highly affected individuals can easily lead to false positives and incorrect generalizations, as well as low power to detect subtle effects across multiple covariate profiles.

Regression-based methods such as [21, 35] allow manual inspection of the coefficients for each covariate interacted with the treatment dummy. However, such approaches typically assume a small number of pre-specified interaction terms and cannot identify other affected subpopulations. The extreme alternative of adjusting for each subpopulation separately, including a term for every possible combination of covariates interacted with the treatment, would require exponentially many interaction terms, leading to computational intractability as well as statistical challenges (lack of power and multiple testing).

Finally, methods such as causal trees [7] and interaction trees [34] use a greedy top-down approach to create specific partitions of the covariate space (the leaves of the tree) that can be interpreted as subpopulations, enabling manual or automatic identification of those partitions with the largest treatment effects. However, when the affected subpopulation and effect size are small, we do not expect the resulting partitions to correspond well to the subpopulation of interest, since the approach optimizes a global objective function such as statistical risk (average loss) rather than focusing on the most significantly affected subpopulations. This difference in emphasis may allow the tree to precisely estimate treatment effects across the entire population (including effects which are near zero) but have larger errors for the small and significantly affected subpopulations we wish to detect: poor choice of partitions could exclude the affected subpopulation from being considered or identified, and instead estimate an effect which is the average over this subpopulation of interest and others. These aspects lead to reduced detection power and accuracy in practice, as shown in our results below. Moreover, the instability of tree-based methods may call into question the relevance of the tree-selected subpopulations, while extensions to random forest-based approaches [40] sacrifice the ability to identify subpopulations for more stable and more accurate estimation of individual treatment effects.

In summary, the current state of the heterogeneous treatment effects literature has many gaps: the only effects of interest are mean shifts, these effects are estimated under possibly restrictive modeling assumptions, only a subset of possible subpopulations are considered and represented, discovering the subpopulation with the largest effect requires manual inspection or an exhaustive search over all modeled subpopulations, and there is little guarantee of the optimality of the discovered subpopulations. In contrast, our proposed TESS approach directly searches for the most significantly affected subpopulations, where significance is measured based on the divergence between the empirical distributions of the treatment and control data, thus avoiding restrictive modeling assumptions. We derive statistical theory which provides performance guarantees, and demonstrate state-of-the-art empirical performance on both real and simulated data, as described below.

### 3 Framework for Distributional Causal Inference

The Treatment Effect Subset Scan framework builds on the widely studied potential outcomes framework (Neyman-Rubin Causal Model), with random treatment assignment, enabling valid causal statements. More

precisely, it begins with observing  $\mathcal{N}$ , a sample of  $n$  independent and identically distributed units from a population of interest  $\mathcal{P}$ . The units are indexed by  $i \in \{1, \dots, n\}$ , and for each unit there is a binary assignment indicator  $W_i \in \{0, 1\}$ , where  $W_i = 0$  indicates assignment to the control group (i.e., the group that did not receive the treatment), while  $W_i = 1$  indicates assignment to the treatment group. Therefore, there exist two potential outcomes for each unit ( $Y_i(0), Y_i(1) \in \mathbb{R}$ ), although only one of these two potential outcomes is observed for each unit. Additionally, each unit is described by  $X_i$ , a  $d$ -dimensional vector of covariates which are fixed, known, and unaffected by treatment assignment. Given this sample, we wish to perform causal inference for the (potentially infinite) population  $\mathcal{P}$ . In particular, there is interest in a causal population estimand that is a function of the potential outcome distributions and covariates:  $\tau = \tau(F_{Y(1)}, F_{Y(0)} | X)$ , which can be approximated with estimators of the finite sample. In particular, we follow the literature and consider finite sample estimators that can be described as row-exchangeable functions of the potential outcomes, treatment assignments, and covariates, for all of the units in  $\mathcal{N}$ . More specifically, we consider  $\tilde{\tau} = \tilde{\tau}(\mathbf{Y}(0), \mathbf{Y}(1), \mathbf{X}, \mathbf{W})$ , where  $\mathbf{Y}(0)$  and  $\mathbf{Y}(1)$  are the  $n$ -dimensional column vectors of potential outcomes,  $\mathbf{W}$  is the  $n$ -dimensional column vector of treatment assignments, and  $\mathbf{X}$  is the  $n \times d$  matrix of covariates, all of which are indexed by sample units  $i$ . In the following subsections we will describe causal estimands that are common in the literature and present the new causal estimands and estimators at the core of our TESS framework.

### 3.1 Causal Estimands in the Literature

The most common estimand in the literature is the average treatment effect (ATE),

$$\tau_{ATE} = \int y \, dF_{Y(1)}(y) - \int y \, dF_{Y(0)}(y) = \mathbb{E}[Y(1) - Y(0)],$$

which computes the expected difference between the potential outcomes across the entire population. Although this summary value is useful, it can be limited when the treatment effect is heterogeneous, or more precisely, where the population's distributions of potential outcomes are dependent on the characteristics of the individual units. The *conditional* average treatment effect (CATE) was introduced for the purposes of relaxing this assumption, considering the potential outcome distributions for each profile of observed characteristics (covariates)  $X = \{X^1, \dots, X^d\}$ . For each covariate profile  $x$ , the CATE is defined as

$$\tau_{CATE}(x) = \int y \, dF_{Y(1)|X}(y|x) - \int y \, dF_{Y(0)|X}(y|x) = \mathbb{E}[Y(1) - Y(0)|X = x],$$

or the expected difference in the potential outcomes for those in the population with covariate profile  $x$ . [19] recently proposed the more flexible marginal conditional average treatment effect (MCATE), defined as

$$\begin{aligned} \tau_{MCATE}(x^s) &= \int \left( \int y \, dF_{Y(1)|X^s}(y|x^s) - \int y \, dF_{Y(0)|X^s}(y|x^s) \right) dF_{X^{-s}|X^s=x^s} \\ &= \int \mathbb{E}[Y(1) - Y(0) | (X^1, X^2, \dots, X^s = x^s, \dots, X^d)] dF_{X^{-s}|X^s=x^s} \\ &= \mathbb{E}[Y(1) - Y(0) | X^s = x^s] \end{aligned}$$

which estimates the expected difference in potential outcomes for the specific subset  $x^s$  of the covariate profile, marginalized over the remaining unfixed covariates. Essentially, MCATE is a weighted average of the CATEs that include  $X^s = x^s$ , weighted by the conditional distribution of the remaining unfixed covariates.

### 3.2 A Distributional Average Treatment Effect Estimand Class

Although MCATE is a generalization of estimands from the literature, it is limited to estimating the average treatment effect for a particular covariate profile  $X^s = x^s$ . In order to provide a population-level measurement that can capture more general changes in the outcome distribution resulting from treatment,

we generalize MCATE to the distributional average treatment effect (DATE), a new class of treatment effect estimands. First, for a given covariate profile  $X = x$ , we define  $\tau_{\text{DATE}}(x)$  as an arbitrary function of the cumulative distribution functions (cdfs) of the potential outcomes  $Y(1)$  and  $Y(0)$  given  $X = x$ :  $\tau_{\text{DATE}}(x) \equiv \tau(F_{Y(1)|X=x}, F_{Y(0)|X=x})$  is a scalar which captures the individual-level treatment effect for a covariate profile  $x$ . For a set of covariate profiles  $S$ , we define  $\tau_{\text{DATE}}(S)$  as a weighted average over the individual profiles:

$$\tau_{\text{DATE}}(S) = \int_{x \in S} \tau_{\text{DATE}}(x) P(X = x \mid X \in S) dx. \quad (1)$$

We note that  $\tau_{\text{CATE}}(x)$  and  $\tau_{\text{MCATE}}(x^s)$  are special cases of  $\tau_{\text{DATE}}(x)$  and  $\tau_{\text{DATE}}(S)$  respectively, with function  $\tau(F_1, F_0) = \int y dF_1(y) - \int y dF_0(y)$ , the difference between the means of the two cdfs, and  $S = \{X : X^s = x^s\}$  consisting of those profiles with the given values for the subset of covariates  $X^s$ . Although the DATE class includes CATE and MCATE, it provides more flexible estimation of treatment effects by allowing other specifications of  $\tau(F_1, F_0)$  that capture arbitrary comparisons between the potential outcome distributions. DATE also provides a flexible definition of subpopulations, considering an arbitrary set  $S$  of covariate profiles, while MCATE only considers a single value  $x$  for each covariate  $X \in X^s$  and all values for each covariate  $X \in X^{-s}$ . Here we consider subsets  $S$  representing *subspaces* of the attribute space, i.e., the Cartesian product of a subset of values for each attribute. This is important because a treatment of interest may affect multiple values, e.g., African-Americans *or* Hispanics who live in New York *or* Pennsylvania.

While  $\tau_{\text{DATE}}(S)$  is useful to estimate for a given subset  $S$ , our primary goal is to identify those subsets  $S$  which have the most significant treatment effects. To do so, we need a model  $H_0$  of how the data is generated under the null hypothesis of no treatment effect, i.e.,  $F_{Y(1)|X=x} = F_{Y(0)|X=x}$  for all  $x$ , and a general measure of divergence,  $\text{Div} : \mathbb{R} \times \mathbb{R} \mapsto \mathbb{R}$ , where  $\text{Div}(u, v) \geq 0$  for all  $u, v$  and  $\text{Div}(u, u) = 0$  for all  $u$ . We then define  $\mu_{\text{DATE}}(S)$  to represent the divergence between  $\tau_{\text{DATE}}(S)$  and its expected value under  $H_0$ :

$$\mu_{\text{DATE}}(S) = \text{Div}(\tau_{\text{DATE}}(S), \mathbb{E}_{H_0}[\tau_{\text{DATE}}(S)]). \quad (2)$$

For MCATE, we note that  $\mathbb{E}_{H_0}[\tau_{\text{MCATE}}(S)] = 0$ , and thus  $\mu_{\text{MCATE}}(S) = \text{Div}(\tau_{\text{MCATE}}(S), 0)$ . As is described in §3.5, the choice of divergence function will depend on our assumptions about the data distribution under both null and alternative hypotheses.

### 3.3 The Nonparametric Average Treatment Effect Estimand

The class of estimands defined by the DATE is large; therefore, we select an instance of this class—which we define as the nonparametric average treatment effect (NATE)—that utilizes the flexibility provided by the DATE to evaluate a general divergence between two potential outcome distributions. We first define

$$\begin{aligned} \tau_{\text{NATE}_\alpha}(x) &= \beta_x(\alpha) \\ &:= F_{Y(1)|X=x}^{-1}(F_{Y(0)|X=x}^{-1}(\alpha)), \end{aligned} \quad (3)$$

which maps the quantile value  $\alpha$  of the control potential outcome distribution into the corresponding quantile value  $\beta$  of the treatment potential outcome distribution. The corresponding  $\tau_{\text{NATE}_\alpha}(S)$  and  $\mu_{\text{NATE}_\alpha}(S)$  are defined as in (1) and (2) respectively. Under  $H_0$  the potential outcomes are equal, thus  $\tau_{\text{NATE}_\alpha}(x) = F_{Y(0)|X=x}^{-1}(F_{Y(0)|X=x}^{-1}(\alpha)) = \alpha$ , and

$$\mu_{\text{NATE}_\alpha}(S) = \text{Div} \left( \int_{x \in S} \beta_x(\alpha) P(X = x \mid X \in S) dx, \alpha \right). \quad (4)$$

Intuitively,  $\mu_{\text{NATE}_\alpha}(S)$  is a comparison between potential outcome distribution functions, localized to a specific subpopulation  $S$  and quantile value  $\alpha$  of the null distribution.

We can also consider the quantity  $\mu_{\text{NATE}}(S) = \max_\alpha \mu_{\text{NATE}_\alpha}(S)$ , which maximizes the divergence between treatment and control potential outcome distributions over the range of quantile values  $\alpha$ . This

estimand will identify arbitrary effects of a treatment, over general subpopulations, measured by the maximal divergence between potential outcome distributions. An additional, and critical, component of NATE is allowing the different covariate profiles  $x \in S$  to have different reference distributions: the distribution  $F_{Y(0)|X=x}$  serves as the expectation for the corresponding distribution  $F_{Y(1)|X=x}$ . We note that the alternative approach of using a single reference distribution, aggregated from all controls in  $S$ , fails when the different covariate profiles being aggregated have different outcome distributions. In this case, marginalization could obfuscate, or even reverse, the true effects that are occurring in these covariate profiles: this phenomena is commonly known as Simpson's Paradox. NATE avoids this paradox by evaluating the relationship between the outcome distributions for individual covariate profiles before aggregating across the subpopulation.

### 3.4 Causal Estimators

Given that the estimands  $\tau_{\text{DATE}}$  and  $\mu_{\text{DATE}}$  are defined in terms of the cumulative distribution functions  $F_{Y(T)|X=x}$ ,  $T \in \{0, 1\}$ , we consider the corresponding finite sample estimators,  $\hat{\tau}_{\text{DATE}}$  and  $\hat{\mu}_{\text{DATE}}$ . We assume that each individual unit  $U_i$  is drawn i.i.d. from  $\mathcal{P}$ . A unit can be represented by a 4-tuple,  $U_i = (X_i, Y_i(0), Y_i(1), W_i)$ , where  $X_i$  are covariates,  $Y_i(0)$  and  $Y_i(1)$  represent that unit's potential outcomes under control and treatment conditions respectively, and  $W_i \in \{0, 1\}$  is the treatment indicator. We note that  $Y_i^{\text{obs}} = Y_i(W_i)$  is the unit's observed outcome, while  $Y_i(1 - W_i)$  is unobserved. We define

$$\hat{F}_{Y^C|X=x}(y) = \frac{\sum_{U_i:X_i=x} \mathbb{1}\{W_i=0\} \mathbb{1}\{Y_i^{\text{obs}} \leq y\}}{\sum_{U_i:X_i=x} \mathbb{1}\{W_i=0\}},$$

and  $\hat{F}_{Y^T|X=x}(y)$  similarly for units with  $W_i = 1$ . These represent the empirical cumulative distribution functions of  $Y_i^{\text{obs}}$  for control individuals with  $X_i = x$  and for treatment individuals with  $X_i = x$  respectively. We can then define:

$$\begin{aligned} \hat{\tau}_{\text{DATE}}(x) &= \tau(\hat{F}_{Y^T|X=x}, \hat{F}_{Y^C|X=x}), \\ \hat{\tau}_{\text{DATE}}(S) &= \frac{1}{n_S} \sum_{U_i:X_i \in S} \hat{\tau}_{\text{DATE}}(X_i) = \sum_{x \in S} \frac{n_x}{n_S} \hat{\tau}_{\text{DATE}}(x), \\ \hat{\mu}_{\text{DATE}}(S) &= \text{Div}(\hat{\tau}_{\text{DATE}}(S), \mathbb{E}_{H_0}[\hat{\tau}_{\text{DATE}}(S)]), \end{aligned}$$

where  $n_x$  and  $n_S$  are the numbers of individuals  $U_i$  with  $X_i = x$  and  $X_i \in S$  respectively.

We would now like to show that these finite sample estimators possess desirable statistical properties, including unbiasedness, consistency, and fast rates of convergence to the corresponding estimands of interest. First, we note that if both potential outcomes were observed for each unit, the corresponding finite sample estimators  $\hat{F}_{Y(T)|X=x}$  can be easily shown to converge to  $F_{Y(T)|X=x}$ , where  $\hat{F}_{Y(T)|X=x}(y) = \frac{1}{n_x} \sum_{U_i:X_i=x} \mathbb{1}\{Y_i(T) \leq y\}$ . Following well-established theory for empirical distribution functions, we know that:

$$\mathbb{E} \left[ \hat{F}_{Y(T)|X=x}(y) \right] = F_{Y(T)|X=x}(y), \quad (5)$$

$$\| \hat{F}_{Y(T)|X=x} - F_{Y(T)|X=x} \|_{\infty} \xrightarrow{\text{a.s.}} 0, \quad (6)$$

$$P \left( \| \hat{F}_{Y(T)|X=x} - F_{Y(T)|X=x} \|_{\infty} > \epsilon \right) \leq 2e^{-2n_x \epsilon^2}, \epsilon > 0, \quad (7)$$

where (5) establishes that  $\hat{F}_{Y(T)|X=x}(y)$  is unbiased for all  $y$ , following from the observation that  $\mathbb{1}\{Y_i(T) \leq y\} \sim \text{Bernoulli}(F_{Y(T)|X=x}(y))$ ; (6) implies that  $\hat{F}_{Y(T)|X=x}$  is strongly consistent, following from the Glivenko-Cantelli Theorem [17]; and (7) implies that convergence rate is exponential in sample size, following [13].

However, the challenge of valid inference, using  $\hat{F}_{Y^C}$  and  $\hat{F}_{Y^T}$  rather than  $\hat{F}_{Y(0)}$  and  $\hat{F}_{Y(1)}$ , remains because at most one of the potential outcomes is observed for each sample: the former quantities are based on observed outcomes only, while the latter quantities are based on both observed and unobserved potential outcomes. To show that  $\hat{F}_{Y^C}$  and  $\hat{F}_{Y^T}$  are unbiased estimators of  $F_{Y(0)}$  and  $F_{Y(1)}$  requires additional

assumptions about the mechanism by which units are assigned to the treatment or control group. Recall that  $W_i$  determines which potential outcome is observed for unit  $U_i$ . If  $W_i$  is biased in which units it assigns to treatment, then subsequent inferences that do not account for this bias may be inaccurate. Thus we assume unconfoundedness:  $Y_i(0), Y_i(1) \perp\!\!\!\perp W_i | X_i$ , i.e., potential outcomes are independent of treatment assignment conditional on the covariates. As a consequence, we show in Lemma 1 that  $\mathbb{E} [\hat{F}_{Y^C|X=x}(y)] = F_{Y(0)|X=x}(y)$ , and similarly  $\mathbb{E} [\hat{F}_{Y^T|X=x}(y)] = F_{Y(1)|X=x}(y)$ . Therefore, given a randomized experiment, the empirical cumulative distribution of the control group is an unbiased and strongly consistent estimator of its population cumulative distribution function, and likewise for the treatment group. Noting that  $\frac{n_x}{n_S} \xrightarrow{a.s.} \mathbb{E} [\frac{n_x}{n_S}]$  and  $\mathbb{E} [\frac{n_x}{n_S}] = P(X = x | X \in S)$ , it follows that  $\hat{\tau}_{\text{DATE}}(x)$ ,  $\hat{\tau}_{\text{DATE}}(S)$ , and  $\hat{\mu}_{\text{DATE}}(S)$ , defined in terms of  $\hat{F}_{Y^T|X=x}$  and  $\hat{F}_{Y^C|X=x}$  as above, are unbiased and strongly consistent finite sample estimators of their population estimands.

### 3.5 Choice of divergence function and test statistic

Having defined the finite sample estimator  $\hat{\mu}_{\text{DATE}}(S)$  in terms of the divergence  $\text{Div}(\cdot, \cdot)$  between  $\hat{\tau}_{\text{DATE}}(x)$  and its expectation under the null hypothesis, we now consider the choice of divergence function. For the non-parametric average treatment effect estimator, recall that  $\hat{\mu}_{\text{NATE}}(S) = \max_{\alpha} \hat{\mu}_{\text{NATE}_{\alpha}}(S) = \max_{\alpha} \text{Div}(\hat{\tau}_{\text{NATE}_{\alpha}}(S), \alpha)$ , where  $\hat{\tau}_{\text{NATE}_{\alpha}}(x) = \hat{F}_{Y^T|X=x}(\hat{F}_{Y^C|X=x}^{-1}(\alpha))$  maps the  $\alpha$  quantile of the control observations with  $X = x$  to a corresponding quantile  $\beta_x(\alpha)$  of the treatment observations with  $X = x$ .

One way to compute  $\hat{\tau}_{\text{NATE}_{\alpha}}(x)$  is to obtain the empirical p-value  $p_i = \hat{F}_{Y^C|X=x}(y_i)$  for each observation  $i$  in the treatment group, comparing its outcome to the reference distribution estimated from the control group, and then to compute the proportion of treatment observations  $n_{\alpha}(x)/n(x)$  with  $p_i < \alpha$ . When sample sizes are small, a more robust estimate can be computed using p-value ranges, as described in §4.2 below.

We now consider two different models of the data generating process, based on the binomial distribution and a normal approximation to the binomial respectively. In each case, we compute the log-likelihood ratio statistic  $F(S) = \log \left( \frac{P(\text{Data}|H_1(S))}{P(\text{Data}|H_0)} \right)$ , which can be written as the product of the total number of p-values  $N(S)$  in subset  $S$  and a divergence  $\text{Div} \left( \frac{N_{\alpha}(S)}{N(S)}, \alpha \right)$  between the observed and expected proportions of p-values that are significant at level  $\alpha$ . For the binomial model, we have:

$$\begin{aligned} H_0 : n_{\alpha}(x) &\sim \text{Binomial}(n(x), \alpha) \quad \forall x \\ H_1(S) : n_{\alpha}(x) &\sim \text{Binomial}(n(x), \beta) \quad \forall x \in S \quad \beta \neq \alpha, \end{aligned}$$

with the following Berk-Jones (BJ) log-likelihood ratio statistic [9, 28]:

$$\begin{aligned} F_{\alpha}^{BJ}(S) &= \log \left[ \frac{P(\text{Data}|H_1(S))}{P(\text{Data}|H_0)} \right] \\ &= N_{\alpha}(S) \log \left( \frac{\beta}{\alpha} \right) + (N(S) - N_{\alpha}(S)) \log \left( \frac{1 - \beta}{1 - \alpha} \right) \\ &= N(S) \text{Div}_{KL} \left( \frac{N_{\alpha}(S)}{N(S)}, \alpha \right), \end{aligned}$$

where we have used the maximum likelihood estimate  $\beta = \beta_{\text{mle}}(S) = \frac{N_{\alpha}(S)}{N(S)}$ , and  $\text{Div}_{KL}(\cdot, \cdot)$  is the Kullback-Liebler divergence,  $\text{Div}_{KL}(x, y) = x \log \frac{x}{y} + (1 - x) \log \frac{1 - x}{1 - y}$ .

For the normal approximation, we have:

$$\begin{aligned} H_0 : n_{\alpha}(x) &\sim \text{Gaussian}(n(x)\alpha, \alpha(1 - \alpha)n(x)) \quad \forall x \\ H_1(S) : n_{\alpha}(x) &\sim \text{Gaussian}(n(x)\beta, \alpha(1 - \alpha)n(x)) \quad \forall x \in S \quad \beta \neq \alpha, \end{aligned}$$

with the following normal approximation (NA) log-likelihood ratio statistic:

$$\begin{aligned}
F_{\alpha}^{NA}(S) &= \log \left[ \frac{P(\text{Data}|H_1(S))}{P(\text{Data}|H_0)} \right] \\
&= \frac{N_{\alpha}(S)(\beta - \alpha)}{\alpha(1 - \alpha)} + \frac{N(S)(\alpha^2 - \beta^2)}{2\alpha(1 - \alpha)} \\
&= \frac{(N_{\alpha}(S) - N(S)\alpha)^2}{2N(S)\alpha(1 - \alpha)} \\
&= N(S) \text{Div}_{\frac{1}{2}\chi^2} \left( \frac{N_{\alpha}(S)}{N(S)}, \alpha \right),
\end{aligned}$$

where we have again used the maximum likelihood estimate of  $\beta = \frac{N_{\alpha}(S)}{N(S)}$ , and  $\text{Div}_{\frac{1}{2}\chi^2}(\cdot, \cdot)$  is a scaled  $\chi^2$  divergence,  $\text{Div}_{\frac{1}{2}\chi^2}(x, y) = \frac{(x-y)^2}{2y(1-y)}$ . The above  $\text{Div} \left( \frac{N_{\alpha}(S)}{N(S)}, \alpha \right)$  each represent a  $\hat{\mu}_{\text{NATE}_{\alpha}}(S)$ , exhibiting the desirable properties described in §3.4, and the corresponding score functions can be written as  $F_{\alpha}(S) = N(S)\hat{\mu}_{\text{NATE}_{\alpha}}(S)$ .

## 4 Treatment Effect Subset Scanning

Treatment Effect Subset Scan (TESS) is a novel framework for identifying subpopulations in a randomized experiment which experience treatment effects—i.e., changes in their outcome distribution—built atop the framework for distributional causal inference established in §3, with the divergence estimand of interest described in §3.3. Unlike previous methods, TESS structures the challenge of treatment effect identification as an anomalous pattern detection problem—where the objective is to identify patterns of systematic deviations away from expectation—which is then solved by scanning over subpopulations. TESS therefore searches for subsets of values of each attribute for which the distributions of outcomes in the treatment groups are systematically anomalous—i.e., significantly different from their expectation as derived from the control group. More precisely, we define a real-valued outcome of interest  $Y$  and a set of discrete covariates  $X = (X^1, \dots, X^d)$ , where each  $X^j$  can take on a vector of values  $V^j = \{v_m^j\}_{m=1 \dots |V^j|}$ . Therefore, we define the arity of covariate  $X^j$  as  $|V^j|$ , the cardinality of  $V^j$ , and note that any covariate profile  $x$ , a realization of  $X$ , follows  $x \in \{V^1 \times \dots \times V^d\}$ . We then define a dataset (as in §3) as a sample  $\mathcal{N}$  composed of  $n$  records (units)  $\{R_1, \dots, R_n\}$ , randomly drawn from population  $\mathcal{P}$ , each of which (indexed by  $i$ ) is described by an outcome  $Y_i$ , covariates  $X_i$ , and an indicator variable  $W_i$ , which indicates if the unit was randomly assigned to the treatment condition; see Table 1 for a demonstrative example. We define the subpopulations  $S$  under consideration to be  $S = \{v^1 \times \dots \times v^d\}$ , where  $v^j \subseteq V^j$ . We wish to find the most anomalous subset

$$S^* = v^{1*} \times \dots \times v^{d*} = \arg \max_S F(S) \quad (8)$$

where  $F(S)$  is commonly referred to in the anomalous pattern detection literature as a score function, to measure the anomalousness of a subset  $S$ . In our work, this function is a test statistic of the treatment effect—i.e., the divergence between the treatment and control group—in subpopulation  $S$  and therefore will be a function of the estimator  $\hat{\mu}_{\text{NATE}}(S)$ .

We accomplish this by first partitioning the experiment dataset into control and treatment groups, and passing the groups to the TESS algorithm. For each unique covariate profile  $x_t$  in the treatment group  $X_t$ , TESS computes the empirical conditional outcome distribution  $\hat{F}_{Y^C|X=x_t}$  from the control group, estimating the conditional outcome distribution under the null hypothesis  $H_0$  that the treatment has no effect on units with this profile. Then for each record  $R_i$  in the treatment group, TESS computes an empirical  $p$ -value range  $p_i$ , which serves as a measure of how uncommon it is to see an outcome as extreme as  $Y_i$  given  $X = x_i$  under  $H_0$ . The ultimate goal of TESS is to discover subpopulations  $S$  with a large amount of evidence against  $H_0$ , i.e., the outcomes of units in  $S$  are consistently extreme given  $H_0$ . Thus TESS searches for subpopulations which contain an unexpectedly large number of low (significant) empirical  $p$ -value ranges, as such a subpopulation is more likely to have been affected by the treatment.

Record	$Y$	$X^{\text{gender}}$	$X^{\text{race}}$	$W$
1	2.35	Female	Black	1
2	2.06	Female	White	1
3	2.92	Male	Black	1
4	2.27	Male	White	1
5	1.73	Female	Black	0
6	1.84	Female	White	0
7	1.7	Male	Black	0
8	1.59	Male	White	0

Table 1: This table is a demonstrative dataset of  $n = 8$  records, with a  $d = 2$  sized vector of covariates,  $X = (X^{\text{gender}}, X^{\text{race}})$ . The first, ( $X^{\text{gender}}$ ), can take values in  $V^{\text{gender}} = \{\text{Female}, \text{Male}\}$ , and the second ( $X^{\text{race}}$ ) can take values in  $V^{\text{race}} = \{\text{Black}, \text{White}\}$ . A covariate profile  $x$ , and realization of  $X$ , is an element in the set of all covariate profiles  $\{V^{\text{race}} \times V^{\text{gender}}\} = \{\{\text{Female}, \text{Black}\}, \{\{\text{Female}, \text{White}\}, \{\{\text{Male}, \text{Black}\}, \{\{\text{Male}, \text{White}\}\}\}\}$ .

## 4.1 Estimating Reference Distributions

After partitioning the data into treatment and control groups, the TESS framework estimates the reference distribution for each unique covariate profile in the treatment group. These estimates follow from two assumptions: randomization and a sharp null hypothesis of no treatment effect. As noted above, randomization implies that  $\hat{F}_{Y^C|X} \xrightarrow{a.s.} F_{Y(0)|X}$ , while the sharp null hypothesis that no subpopulation is affected by the treatment implies that  $F_{Y(0)|X} = F_{Y(1)|X}$ ; therefore, TESS uses  $\hat{F}_{Y^C|X}$  as an unbiased and strongly consistent estimator of the unknown  $F_{Y(1)|X}$  under  $H_0$ . Intuitively, under  $H_0$  the outcomes of the treatment and control groups are drawn from the same distribution, allowing  $\hat{F}_{Y^C|X=x_t}$  to serve as an outcome reference distribution for treatment units with covariate profile  $X = x_t$ . **When  $H_0$  is true** the outcomes for every unit in the treatment group and the control group, with the same covariate profile, are exchangeable. **When  $H_0$  is false** the affected treatment outcomes are drawn from an alternative distribution, different than their assumed reference distributions under  $H_0$ . No additional assumptions are made about the relationship between reference distributions.

## 4.2 Computing Empirical P-value Ranges

TESS calculates empirical  $p$ -value ranges [28] for each treatment unit to obtain a measure of how “anomalous” or unusual a particular unit’s outcome is given its reference distribution. For each unit  $R_t$  in the treatment group, we compute its empirical reference distribution:

$$\hat{F}_{Y^C|X}(y_t|x_t) = \frac{1}{n(x_t)} \sum_{Y_i \in Y^C(x_t)} \mathbb{1}\{Y_i \leq y_t\}, \quad (9)$$

where  $Y^C(x_t)$  is the set of outcomes for control units with covariate profile  $x_t$  and  $n(x_t) = |Y^C(x_t)|$ . Observe that the standard empirical  $p$ -value would be  $\hat{p}(y_t; x_t) = \hat{F}_{Y^C|X}(y_t|x_t)$ . The empirical  $p$ -value range is essentially a decomposition of this traditional empirical  $p$ -value with the  $p$ -value range corresponding to treatment unit  $R_t$  defined as

$$\begin{aligned} p_t &= [p_{\min}(p_t), p_{\max}(p_t)] \\ &= \left[ \frac{\sum_{Y_i \in Y^C(x_t)} \mathbb{1}\{Y_i < y_t\}}{n(x_t) + 1}, \frac{\left( \sum_{Y_i \in Y^C(x_t)} \mathbb{1}\{Y_i \leq y_t\} \right) + 1}{n(x_t) + 1} \right]. \end{aligned} \quad (10)$$

The additional  $+1$  in the denominator of both  $p_{\min}$  and  $p_{\max}$  and the numerator of  $p_{\max}$  follows from the exchangeability of the outcomes under  $H_0$ . Moreover, we use empirical  $p$ -value ranges because they improve upon traditional empirical  $p$ -values: most importantly, empirical  $p$ -value ranges are distributed Uniform[0,1]—also following from exchangeability and the probability integral transform—while traditional empirical  $p$ -values are only asymptotically distributed Uniform[0,1]. As a result, the ranges are unbiased

		Gender	
		Male	Female
Race	Black	{1.7}	{1.73}
	White	{1.59}	{1.84}

		Gender	
		Male	Female
Race	Black	{2.92}	{2.35}
	White	{2.21}	{2.06}

Control Group

Treatment Group

Table 2: This table is a demonstrative tensor—representing the example dataset in Table 1—containing a  $d = 2$ -order tensor for both the control and treatment group. The top-left cell of each tensor represents the subpopulation of black males in the data  $S = \{\{\text{Black}\} \times \{\text{Male}\}\}$ . There are also the subpopulation of all males ( $S = \{\{\text{Black}, \text{White}\} \times \{\text{Male}\}\}$ ), all black subjects ( $S = \{\{\text{Black}\} \times \{\text{Male, Female}\}\}$ ), or the entire population ( $S = \{\{\text{Black}, \text{White}\} \times \{\text{Male, Female}\}\}$ ); there are a total of nine subpopulations in this simple example. We note that the example dataset has only one unit with each unique covariate profile, therefore the set of values in each tensor cell is of size one.

(Lemma 2) while traditional empirical  $p$ -values exhibit finite sample bias from non-uniformity and the potential bias that could result from tied outcomes. We note that (10) is defined in terms of left-tailed  $p$ -value ranges, which identify values in the extremes of the lower-tail of the reference distribution. The  $p$ -value range in relation to the right-tail is  $p_t = [1 - p_{\max}(p_t), 1 - p_{\min}(p_t)]$ . We define the significance of a  $p$ -value range, for a significance level  $\alpha$ , as

$$n_\alpha(p_t) = \begin{cases} 1 & \text{if } p_{\max}(p_t) < \alpha \\ 0 & \text{if } p_{\min}(p_t) > \alpha \\ \frac{\alpha - p_{\min}(p_t)}{p_{\max}(p_t) - p_{\min}(p_t)} & \text{otherwise.} \end{cases}$$

Intuitively,  $n_\alpha(p_t)$  measures the amount of the range that is significant at  $\alpha$ , or equivalently, the probability that a  $p$ -value drawn uniformly from  $[p_{\min}(p_t), p_{\max}(p_t)]$  is less than  $\alpha$ .

Finally, although we define and estimate (9) individually for each covariate profile  $x_t$  using the empirical distribution function, we note that our framework only requires a means to compute a  $p$ -value (range) for each treatment unit. The empirical distribution allows TESS to accommodate arbitrary differences in the conditional outcomes distributions across covariate profiles enabling general applicability without a priori knowledge of the context of interest. However, in a specific context, it may be possible to exploit reasonable assumptions and construct a better estimator. Additionally, when the covariate profiles contained in the affected subpopulation(s) constitute a small number of control units, it may prove more efficient to learn a more general estimate (combining data across profiles) of the conditional probability distributions. Statistical learning offers many options for density estimation, any of which can be utilized in TESS.

### 4.3 Subpopulations

Given  $p$ -value ranges as a measure of the anomalousness of individual treatment units, we now consider how TESS combines these measures forming subpopulations. For intuition, we propose representing the data as a tensor, where each covariate is represented by a mode of the tensor,  $X = (X^1, \dots, X^d)$  resulting in a  $d$ -order tensor,  $|V^j|$  (the arity of the  $j^{th}$  covariate) is the size of the  $j^{th}$  mode. Therefore, each covariate profile  $x$  maps to a unique cell in the tensor, which contains the  $p$ -values of the treatment units that share  $x_t$  as their covariate profile. As stated above, a subpopulation is  $S = \{v^1 \times \dots \times v^d\}$ , where  $v^j \subseteq V^j$ ; therefore, an individual cell is itself a subpopulation:  $S = \{\{x^1\} \times \dots \times \{x^d\}\}$ . For a demonstrative example see Table 2. For a given subpopulation  $S$ , we define the quantities

$$C(S) = \bigcup_{x_t \in S} Y^T(x_t), \quad N_\alpha(S) = \sum_{p_t \in C(S)} n_\alpha(p_t), \quad N(S) = \sum_{p_t \in C(S)} 1 \quad (11)$$

where  $Y^T(x_t)$  is defined similarly to  $Y^C(x_t)$ , but for the treatment group;  $C(S)$  is the union of the cells (i.e., covariate profiles) in  $S$ , and the  $p$ -value ranges they contain;  $N(S)$  represents the total number of empirical  $p$ -value ranges contained in  $C(S)$ ; and  $N_\alpha(S)$  is the total probability mass less than  $\alpha$  in these  $p$ -value ranges. Under the null hypothesis  $H_0$  that the treatment has no effect, the distribution of each  $p$ -value range is Uniform[0,1]. Therefore, for a subpopulation  $S$  consisting of  $N(S)$  empirical  $p$ -value ranges,

$\mathbb{E}[N_\alpha(S)] = \alpha N(S)$ , which follows from Lemma 2: empirical  $p$ -values are distributed Uniform[0,1] under  $H_0$ . Under the alternative hypothesis, we expect the outcomes of the affected units to be more concentrated in the tails of their reference distributions; thus, the  $p$ -value ranges for these affected units will be lower. Therefore, subpopulations composed of covariate profiles that are systematically affected by the treatment should express higher values of  $N_\alpha(S)$  for some  $\alpha$ . Consequently, a subpopulation  $S$  where  $N_\alpha(S) > \alpha N(S)$  (i.e., with a higher than expected number of low, significant  $p$ -value ranges) is potentially affected by the treatment.

## 4.4 Nonparametric Scan Statistic

TESS utilizes the nonparametric scan statistic [28] to evaluate the statistical anomalousness of a subpopulation  $S$  by comparing the observed and expected number of significantly low  $p$ -value ranges it contains. The general form of the nonparametric scan statistic is

$$F(S) = \max_{\alpha} F_\alpha(S) = \max_{\alpha} \phi(\alpha, N_\alpha(S), N(S)) = \max_{\alpha} N(S) \hat{\mu}_{\text{NATE}_\alpha}(S),$$

where  $N_\alpha(S)$  and  $N(S)$  are defined as in (11). Here  $F_\alpha(S)$  is a log-likelihood ratio test statistic of the treatment effect in subpopulation  $S$  which, as shown in §3.5, is proportional to the divergence  $\hat{\mu}_{\text{NATE}_\alpha}(S)$ . We consider “significance levels”  $\alpha$  between 0 and some constant  $\alpha_{\max} \leq 1$ . Selecting  $\alpha_{\max}$  in conjunction with the tail(s) of interest, describes which quantiles of the reference distribution outcomes must fall into in order to be considered significant. Maximizing  $F(S)$  over a range of  $\alpha$ , rather than a single arbitrarily-chosen  $\alpha$  value, enables TESS to detect a small number of highly anomalous  $p$ -value ranges, a larger subpopulation with subtly anomalous  $p$ -values, or anything in between.

### 4.4.1 Efficient Scanning

The next step in the TESS framework is to detect the subpopulation most affected by the treatment, i.e., to identify the most anomalous subset of values for each of the  $d$  modes of the tensor, or equivalently for each covariate  $X^1 \dots X^d$ . More specifically, the goal is to identify the set of subsets  $\{v^1, \dots, v^d\}$  where each element corresponds to values in a tensor-mode (covariate), such that  $F(\{v^1 \times \dots \times v^d\})$  is jointly maximized.

The computational complexity of solving this optimization naively is  $O(2^{\sum_j |V^j|})$ , where  $|V^j|$  is the size of mode  $j$  (the arity of  $X^j$ ), and is computationally infeasible for even moderately sized datasets. [29] defines the linear-time subset scanning (LTSS) property, which allows for efficient and exact maximization of any function satisfying LTSS over all subsets of the data; more specifically, [29] proposes weak- and strong-LTSS, where strong-LTSS implies weak-LTSS. [28] demonstrated that the nonparametric scan statistic satisfies strong-LTSS when the given dataset is defined by a set of data records  $R_1 \dots R_n$  and attributes  $A_1 \dots A_d$ , and the optimization of a nonparametric scan statistic is over subsets of the form  $S = R \times A$ . In the setting of TESS, data elements are not records but rather  $v_m^j$  (the values of mode  $j$ ) for a given  $j$  and  $m = 1, \dots, |V^j|$ . Therefore, while holding the assignments of the other  $d - 1$  modes constant, we are concerned with finding the optimal  $v^j$  of which there are  $O(2^{|V^j|})$  many to consider. This optimization of the nonparametric scan statistic for tensor modes does not satisfy strong-LTSS; therefore, we demonstrate in Corollary 2 that the nonparametric scan statistic in the context of TESS satisfies weak-LTSS and modes of a tensor can be efficiently optimized. More specifically, first let  $U(S, \alpha_{\max})$  be the set of unique  $\alpha$  values to be considered for subpopulation  $S$ , for  $\alpha_{\max} \in (0, 1)$  and  $|U(S, \alpha_{\max})| \leq n_t$ , recalling that  $n_t$  is the total number of treatment units. Then  $\max_S F(S) = \max_{\alpha \in U(S, \alpha_{\max})} \max_S F_\alpha(S)$ , with priority function  $G_\alpha(v_m^j) = \frac{\sum_{p_t \in C(v_m^j \times v^{-j})} n_\alpha(p_t)}{\sum_{p_t \in C(v_m^j \times v^{-j})} 1}$ , can be efficiently and exactly computed over all subsets  $S = v^j \times v^{-j}$ , where  $v^j \subseteq V^j$ , for a given subset of values for each of the other modes  $v^{-j}$ . To do so, consider the set of distinct  $\alpha$  values  $U = U(V^j \times v^{-j}, \alpha_{\max})$ , and for each  $\alpha \in U$  we can follow a sequence of steps to optimize  $F_\alpha(S)$ : compute the priority  $G_\alpha(v_m^j)$  for each value ( $v_m^j \in V^j$ ), sort the values based on priority, and evaluate subsets  $S = \{v_{(1)}^j \dots v_{(k)}^j\} \times v^{-j}$  consisting of the top- $k$  highest priority values, for  $k = 1, \dots, |V^j|$ .

TESS uses LTSS to efficiently optimize over all subsets of values for a given tensor mode (conditioned on values for the other tensor modes) in its search procedure for maximizing the score function  $F(S)$  over all subpopulations. First we choose, uniformly at random, a subset of values for each mode  $v^1 \subseteq V^1, \dots, v^d \subseteq V^d$ . TESS then iterates over modes of the tensor, using the efficient optimization steps described above to optimize each mode:  $v^j = \arg \max_{v^j \subseteq V^j} F(v^j \times v^{-j}), j = 1 \dots d$ . The cycle of optimizing each mode continues until convergence, at which point TESS has reached a conditional maximum of the score function, i.e.,  $v^j$  is conditionally optimal given  $v^{-j}$  for all  $j = 1 \dots d$ . This ordinal ascent approach is not guaranteed to converge to the joint optimum but with multiple random restarts, this procedure can locate near globally optimal subsets with high probability [28]. Moreover, if  $\sum_{j=1}^d |V^j|$  is large, this iterative procedure makes the ability to detect anomalous subpopulations computationally feasible, without removing subpopulations from the search space (as a greedy top-down approach may). Details of the TESS algorithm and its computational complexity are in the supplemental materials.

## 4.5 Estimator Properties

In the above sections we outline a procedure to efficiently compute  $\max_{S \in R} F(S)$  where  $R$  represents the space of all rectangular subsets. In this section we treat  $\max_{S \in R} F(S)$  as a statistic of the data and aim to show that it has desirable asymptotic properties. The first of these properties is that this test statistic can be used in the following hypothesis test

$$\begin{aligned} H_0 : Y_i(1) &\sim F_{Y_i(0)|X_i} \quad \forall i \\ H_1(S) : Y_i(1) &\not\sim F_{Y_i(0)|X_i} \quad \forall X_i \in S \quad \text{and} \quad Y_i(1) \sim F_{Y_i(0)|X_i} \quad \forall X_i \notin S. \end{aligned}$$

The null hypothesis is that all of the observed outcomes of treatment units are drawn from the same conditional outcome distribution (given the observed covariates) as the control group. Therefore,  $\max_{S \in R} F(S)$  provides a means to quantify the evidence to reject  $H_0$ .

**Theorem 2.** *Let  $n(x_t) \geq n \ \forall x_t \in D$ , i.e., assume that each of the  $M$ -many unique covariate profiles in the data (or cells in the tensor) that are non-empty in both treatment and control, has at least  $n$  data points. Additionally, assume that  $Mn \rightarrow \infty$ , then for some test level  $\gamma \in (0, 1)$  and sequence of critical values  $h(M)$ ,*

$$P_{H_0} \left( \max_{S \in R} F(S) > h(M) \right) \rightarrow 0.$$

Therefore the Type I error rate can be controlled and our statistic produces an asymptotically valid  $\gamma$ -level hypothesis test  $P_{H_0}(\text{Reject } H_0) \leq \gamma$ . Additionally, we can show:

**Theorem 3.** *Let  $n(x_t) \geq n \ \forall x_t \in D$ ,  $S^T$  be the truly affected subset of data, and  $k$  be the proportion of non-empty unique covariate profiles in the data (or cells in the tensor) that are affected under  $H_1(S^T)$ . Additionally, assume  $kMn \rightarrow \infty$ , then*

$$P_{H_1} \left( \max_{S \in R} F(S) > h(M) \right) \rightarrow 1.$$

Therefore the Type II error rate can be controlled and produces a hypothesis test with full asymptotic power,  $P_{H_1}(\text{Reject } H_0) \rightarrow 1$ . This result intuitively captures the statistic's ability to conclude that the null hypothesis is false—i.e., there exist some subset that follows  $H_1$ , and therefore invalidates  $H_0$ . However, this does not necessarily provide a guarantee that the statistic will exactly capture the true subset. Therefore, we introduce (and formally define in the supplementary materials) the concepts of effect *homogeneity*—measuring how similarly the treatment affects each  $F_{Y_i|X_i}$  for  $X_i \in S^T$ —and *strength*—measuring how large of an effect the treatment exhibits across all  $F_{Y_i|X_i}$  for  $X_i \in S^T$ . If we let  $S^* = \arg \max_{S \in R} F(S)$ , these concepts allow for the following result:

**Theorem 6.** Under  $H_1(S^T)$ , where  $S^T$  is a  $t$ -element subset of data elements that are not drawn from the null data generating process, if the alternative process produces an observed signal that is  $\nu$  – homogenous and  $\frac{\delta}{\eta}$  – strong, then  $S^* = S^T$ .

These results provide sufficient conditions under which the highest-scoring subset corresponds exactly to the true affected subset. To our knowledge, this is the first work on heterogeneous treatment effects that provides such conditions on subpopulation exactness.

## 5 Empirical Analysis

In this section we empirically demonstrate the utility of the TESS framework as a tool to identify subpopulations with significant treatment effects. We use data from the Tennessee Student/Teacher Achievement Ratio (STAR)[42] randomized experiment in order to provide representative performance in real-world policy analysis. We review the original STAR data (§5.1), and describe our procedure for simulating affected subpopulations (§5.2).

Through the simulation results described in §5.3, we compare the ability of TESS to detect significant subpopulations to three recently proposed statistical learning approaches: Casual Tree [7], Interaction Tree [7, 34], and Causal Forest [40]. Specifically, we evaluate each method on two general metrics: detection power and subpopulation accuracy. Detection power measures  $P_{H_1}(\text{Reject } H_0)$ , or how well a method can detect the existence—not necessarily the location—of treatment effect heterogeneity in the experiment. Subpopulation accuracy, on the other hand, is specifically designed to measure how well a method can precisely and completely capture the subpopulation(s) with significant treatment effects.

Finally, we conduct an exploratory analysis of the STAR dataset, and in §5.4 discuss the subpopulations identified by TESS as affected by treatments. In some cases, the identified subpopulation is consistent with the literature on the STAR experiment; in other cases, TESS uncovers previously unreported, but intuitive and believable, subpopulations. These empirical results demonstrate TESS’s potential to generate potentially useful and non-obvious hypotheses for further exploration and testing.

### 5.1 Tennessee STAR Experiment

The Tennessee Student/Teacher Achievement Ratio (STAR) experiment is a large-scale, four-year, longitudinal randomized experiment started in 1985 by the Tennessee legislature to measure the effect of class size on student educational outcomes, as measured by standardized test scores. The experiment started monitoring students in kindergarten (during the 1985-1986 school year) and followed students until third grade. Students and teachers were randomly assigned into conditions during the first school year, with the intention for students to continue in their class-size condition for the entirety of the experiment. The three potential experiment conditions were not based solely on class size, but also the presence of a full-time teaching aide: small classrooms (13-17 pupils), regular-size classrooms (22-25 pupils), and regular-size classrooms with aide (still 22-25 pupils). Therefore, the difference between the former two conditions is classroom size, and the difference between the latter two conditions is the inclusion of a full-time teacher’s aide in the classroom. The experiment included approximately 350 classrooms from 80 schools, each of which had at least one classroom of each type. Each year more than 6,000 students participated in this experiment, with the final sample including approximately 11,600 unique students.

The Tennessee STAR dataset has been well studied and analyzed, both by the project’s internal research team [14, 42] and by external researchers [26, 31]. As indicated by [26], the investigations have primarily focused on comparing means and computing average treatment effects. [26] presents a detailed econometric analysis and draws similar conclusions to the previous research: students in small classrooms perform better than those in regular classrooms, while there is no significant effect of a full-time teacher’s aide, or moderation from teacher characteristics. Moreover, the effect accumulates each year a student spends in a small classroom [26]. Additionally, these conclusions are robust in the presence of potentially compromising experimental design challenges: imbalanced attrition, subsequent changes in original treatment assignment, and fluctuating class-sizes [26].

## 5.2 Experimental Simulation Setup

The goal of our experimental simulation is to replicate conditions under which a researcher would want to use an algorithm to discover subpopulations with significant treatment effects, and to observe how capable various algorithms are at identifying the correct subpopulation(s). In order to replicate realistic conditions, we use the STAR experiment as our base dataset, and inject into it subpopulations (of a given size) with a treatment effect (of a given magnitude). More specifically, we treat each student-year as a unique record and for each record capture ten covariates: student gender, student ethnicity, grade, STAR treatment condition, free-lunch indicator, school development environment, teacher degree, teacher ladder, teacher experience, and teacher ethnicity. We note that each of these variables, other than teacher experience, is discrete; we discretize experience into five-year intervals:  $[0, 5), [5, 10), \dots, [30, \infty)$ . The number of values a covariate can take ranges from two to eight. By preserving the overall data structure of the STAR experiment—number of covariates, covariate value correlations, subpopulation, sample sizes, etc.—our simulations are more able to replicate the structure (and challenges) faced by experimenters.

The process we follow to generate a simulated treatment effect begins with selecting a subpopulation  $S_{\text{affected}}$  to affect. Recall that the dataset contains a set of discrete covariates  $X = (X^1, \dots, X^d)$ , where each  $X^j$  can take on a vector of values  $V^j = \{v_m^j\}_{m=1\dots|V^j|}$  and  $|V^j|$  is the arity of covariate  $X^j$ . Therefore, we define a subpopulation as  $S = \{v^1 \times \dots \times v^d\}$ , where  $v^j \subseteq V^j$ . The affected subpopulation is generated at random based on two parameters: *num\_covs*, or the number of covariates to select, and *value\_prob*, or probability a covariate value is selected. We select *num\_covs* covariates at random, and for each of these covariates we select each of their values with probability equal to *value\_prob*, ensuring that at least one value for each of these covariates is selected. The final affected subpopulation is then  $S_{\text{affected}} = \{v^1 \times \dots \times v^d\}$ , where  $v^j$  is the selected values if  $X^j$  is one of the *num\_covs* covariates, and otherwise  $v^j = V^j$ . In other words, for a random subset of covariates,  $S_{\text{affected}}$  only includes a random subset of their values, and for all other covariates  $S_{\text{affected}}$  includes all their values. This treatment effect simulation scheme allows for variation in the size of the subpopulation that is affected: instances of  $S_{\text{affected}}$  can constitute a small subpopulation (a challenging detection task), a large subpopulation (a relatively easier detection task), or something in between. Therefore a set of simulations, with varying parameter values, captures the spectrum of conditions a researcher may face when analyzing an experiment to identify subpopulations with significant treatment effects.

The next step in the process involves partitioning the dataset into treatment and control groups, and generating outcomes for each record. Outcomes are drawn randomly from one of two distributions: the null distribution ( $f_0$ ) or the alternative distribution ( $f_1$ ). Any record in the treatment group that has a covariate profile  $x \in S_{\text{affected}}$  receives outcomes generated by  $f_1$ ; all other records receive outcomes drawn from  $f_0$ . Therefore only  $S_{\text{affected}}$  has a treatment effect, whose effect magnitude is the distributional difference between  $f_0$  and  $f_1$ , which we represent by the parameter  $\delta$ .

Each of the methods we consider in these experiments has a unique approach to identifying potential subpopulations with differential treatment effects. Furthermore, as mentioned in §2.1 most methods in the literature do not provide a process for identifying extreme treatment effects. Therefore, we devise intuitive post-processing steps in an attempt to represent how researchers would use each method to identify potential subpopulations that have significant treatment effects. Each method returns identified subpopulations and corresponding scores (measures) of the treatment effect. For the single tree-based method [7, 34] we follow the suggestion of [7] to perform inference (via a two-sample Welch T-Test) in each leaf of the tree, and we then sort the leaves based on their statistical significance. The final subpopulation returned by the tree is the leaf with the most statistically significant treatment effect, and the final treatment effect measure is this leaf's statistical significance (i.e., p-value). For a method that provides an individual level treatment effect (and estimate of variance) [40], we propose to perform inference for each unique covariate profile, and return those that are statistically significant. The final treatment effect measure is the smallest p-value of the covariate profiles. The TESS algorithm, by design, provides the subpopulation it determines to have a statistically significant distributional change (treatment effect) and a measure of this change, so no post-processing is necessary.

### 5.2.1 Detection Power

For any combination of simulation parameter values  $(\delta, num\_cows, value\_prob)$ , detection power measures  $P(Reject H_0 | H_1(S_{\text{affected}}))$ , or how well a method is able to identify the presence of  $S_{\text{affected}}$ . This is accomplished by comparing the treatment effect measure (score of the detected subset) found under  $H_1(S_{\text{affected}})$  to the distribution of the treatment effect measure under  $H_0$ . More specifically, for a given set of parameter values, we generate a random dataset which only exhibits a treatment effect in the randomly selected subpopulation  $S_{\text{affected}}$ ; each method attempts to detect this subpopulation. As described in §5.2, each method returns a final treatment effect measure for the subpopulation it detects in this affected dataset. For the same dataset, we then conduct randomization testing to determine how significant this treatment effect measure is under  $H_0$ . We make many copies of the dataset (1000 in our experiments) and in each copy, we generate new outcomes (drawn from  $f_0$ ) such that no subpopulation has a treatment effect. Each method then generates a detected subpopulation and corresponding treatment effect measure for each of these null datasets. These treatment effect measures from the null datasets together provide an empirical estimate of the distribution of the treatment effect measure under  $H_0$  for that method. Subsequently, a  $p$ -value is computed for the treatment effect measure captured under  $H_1(S_{\text{affected}})$ . This process is repeated many times (300 in our experiments), where each time we 1) generate a random  $S_{\text{affected}}$ , 2) generate a random dataset under  $H_1(S_{\text{affected}})$  and compute each method's treatment effect measure, and 3) generate 1000 copies of the dataset with no treatment effect to compute each method's treatment effect measure distribution under  $H_0$ . This process creates 300  $p$ -values for each method which describe how extreme each of the  $S_{\text{affected}}$  appear under  $H_0$ . A method rejects  $H_0$  for a given  $p$ -value if it is less than or equal to some test-level  $\gamma$ , corresponding to the  $1 - \gamma$  quantile of the null distribution ( $\gamma = 0.05$  in our experiments). Therefore, the detection power  $P(Reject H_0 | H_1(S_{\text{affected}}))$  is captured as the proportion of  $p$ -values that are sufficiently extreme that they lead to the rejection of  $H_0$  at level  $\gamma$ .

### 5.2.2 Detection Accuracy

While detection power measures how well a method identifies the presence of a subpopulation with a treatment effect  $S_{\text{affected}}$ , as compared to datasets with no treatment effect, detection accuracy measures how well a method can precisely and completely identify the affected subpopulation  $S_{\text{affected}}$ . Accurately identifying in which subpopulation(s) a treatment effect exists can be crucial, particularly when there is no prior theory to guide which subpopulations to inspect, or when the goal itself is to develop intuition for new theory. As described in §5.2, each of the methods we consider is able to return the subpopulation that it determines as having the most statistically significant treatment effect  $S_{\text{detected}}$ . Each method will pick out a set of covariate profiles, which could have coherent structure (as with TESS, Causal Tree, and Interaction Tree), or be an unstructured collection of individually significant covariate profiles (as with Causal Forest). To accommodate both types of subpopulations, we therefore define detection accuracy as

$$\text{accuracy} = \frac{|S_{\text{detected}} \cap S_{\text{affected}}|}{|S_{\text{detected}} \cup S_{\text{affected}}|} = \frac{\sum_{R_t} \mathbb{1}\{R_t \in S_{\text{detected}} \cap S_{\text{affected}}\}}{\sum_{R_t} \mathbb{1}\{R_t \in S_{\text{detected}} \cup S_{\text{affected}}\}}. \quad (12)$$

where  $R_t$  are records in the treatment group. This definition of accuracy, commonly known as the Jaccard coefficient, is intended to balance precision (i.e., what proportion of the detected subjects truly have a treatment effect) and recall (i.e., what proportion of the subjects with a treatment effect are correctly detected). We note that  $0 \leq \text{accuracy} \leq 1$ ; high accuracy values correspond to a detected subset  $S_{\text{detected}}$  that captures many of the subjects with treatment effects and few or no subjects without treatment effects.

## 5.3 Simulation Results

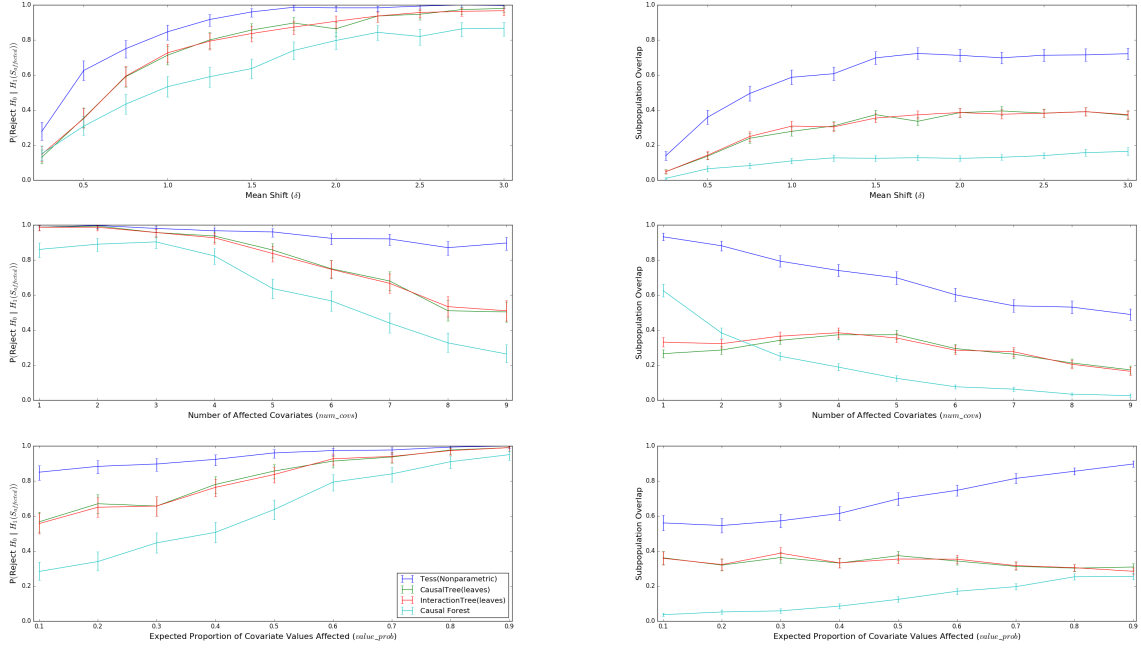
Our first set of results involve a treatment effect that is a mean shift in a normal distribution: the null distribution  $f_0 = N(0, 1)$  and the alternative  $f_1 = N(\delta, 1)$ , where  $\delta$  captures the magnitude of the signal (treatment effect). Recall from §5.2 that there are three parameters that we can vary to change the size and magnitude of the signal. For our simulation, we specifically consider  $\delta \in \{0.25, 0.5, \dots, 3.0\}$ ,  $num\_cows \in$

$\{1, 2, \dots, 10\}$ , and  $value\_prob \in \{0.1, 0.2, \dots, 0.9\}$ ; the former controls magnitude of the treatment effect, while the latter two control the concentration of the treatment effect (i.e., the expected size of the affected subpopulation). Instead of considering every combination, we select the middle value of each parameter interval as a reference point ( $\delta = 1.5$ ,  $num\_coks = 5$ ,  $value\_prob = 0.5$ ) and measure performance changes for one parameter, while keeping the others fixed.

Figure 1a shows the changes in each method's detection power performance as we vary each of the three parameters that contribute to the strength of the treatment effect. From each of the three graphs we observe that TESS consistently exhibits more power than (or equivalent to) the other methods. More importantly, TESS exhibits statistically significant improvements in power for the most challenging ranges of parameter values (i.e., more subtle signals). The top plot varies effect size (or  $\delta$ ), which is positively associated with signal strength and negatively associated with detection difficulty; for values 2.0 and below TESS has significantly higher detection power than the competing methods. The middle plot varies the number of covariates selected to have only a subset of values be affected ( $num\_coks$ ). This parameter is negatively associated with signal strength and positively associated with detection difficulty; for values 5 and above, TESS has significantly higher detection power. The bottom plot varies the expected proportion of values, for the selected covariates, which will be affected ( $value\_prob$ ). This parameter is positively associated with signal strength and negatively associated with detection difficulty; for values 0.5 and below TESS exhibits significantly higher detection power. We see that, for sufficiently strong signals (based on both signal magnitude and concentration), all methods are able to distinguish between experiments with and without a subpopulation exhibiting a treatment effect, while TESS provides significant advantages in detection power for weaker signals. Figure 1b shows the changes in each method's detection accuracy as we vary each of the three parameters that contribute to the strength of the treatment effect. From each of the three graphs we observe that TESS consistently exhibits significantly higher accuracy than any other method. Recall that we measure subpopulation accuracy as in (12), which captures both precision and recall of the subpopulation returned by a method. The single tree methods tend to have high precision but low recall, resulting in compromised overall accuracy. Intuitively, these results indicate that the truly affected subpopulation is being spread over multiple leaves of the tree, despite its goal of partitioning the data into subpopulations with similar outcomes. This phenomenon may be caused by the greedy search aspect of tree learning: if the tree splits the affected subpopulation between two branches of the tree, the recall of any leaf will be compromised, especially when this split occurs close to the root of the tree. The Causal Forest ensemble method, on the other hand, exhibits relatively higher recall than precision. These results indicate that it is difficult for Causal Forest to distinguish between the covariate profiles that do and do not make up the truly affected subpopulation, as profiles from both sets appear to have statistically significant treatment effects. This inability stems from the fact that ensemble methods are designed to provide individual level predictions, therefore the conclusions drawn on the statistical significance of a covariate profile is done in isolation of the other covariate profiles that also make up the affected subpopulation. Unlike single-tree methods, ensemble methods do not provide coherent and natural groupings of subpopulations. TESS, however, does provide a coherent subpopulation, which seems to balance precision and recall, maintaining a significantly higher subpopulation accuracy.

It is also important to note that the data generating process for these simulations (a treatment effect that occurs as a mean shift between treatment and control distributions) corresponds to the modeling assumptions of the current methods in the literature, which specifically attempt to detect mean shifts, while TESS is designed to detect more general distributional changes. TESS's improved performance, as compared to the competing methods, in these adverse conditions may be due to its subset-scanning based approach, which combines information across groups of data in an attempt to find exactly and only the affected subset of data. Even if each individual covariate profile that is truly affected exhibits small evidence of a treatment effect, TESS can leverage the group structure and signal of all the affected covariate profiles, and correctly conclude that collectively the subpopulation exhibits significant evidence of a treatment effect. Additionally, the fact that TESS executes its optimization iteratively, unlike the greedy search of tree-based methods, enables it to rectify initial choices of subset that are later determined to be inferior.

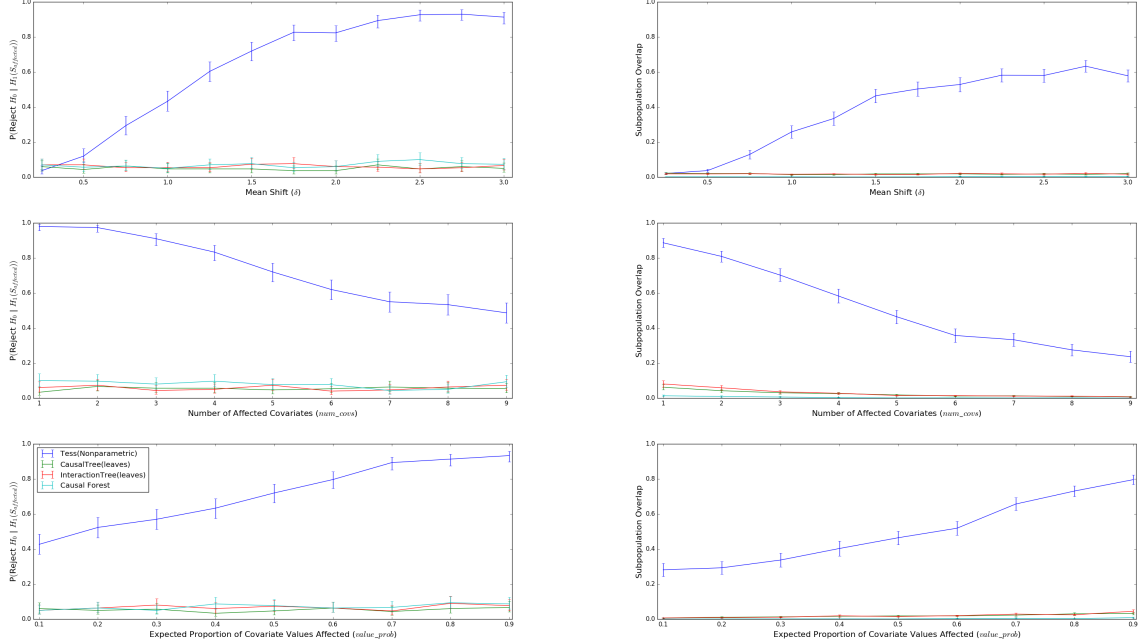
Our second set of results consider treatment effects that do not align with the mean shift assumption



(a) Detection Power

(b) Detection Accuracy

Figure 1: Ability of each method to identify subpopulations with mean shift treatment effects. The three parameters start as fixed ( $\delta = 1.5$ ,  $num\_cows = 5$ ,  $value\_prob = 0.5$ ) and then are varied individually to see how detection ability varies.



(a) Detection Power

(b) Detection Accuracy

Figure 2: Ability of each method to identify subpopulations with an unaffected mean, but distributional treatment effect. The three parameters start as fixed ( $\delta = 1.5$ ,  $num\_cows = 5$ ,  $value\_prob = 0.5$ ) and then are varied individually to see how detection ability varies.

that pervades the literature. Therefore, the null distribution is still  $f_0 = N(0, 1)$ , however the alternative is a mixture distribution  $f_1 = \frac{1}{2}N(-\delta, 1) + \frac{1}{2}N(\delta, 1)$ . Here  $\delta$  still captures the magnitude of the signal (treatment effect), and the remainder of the simulation process remains unchanged. This mixture distribution alternative, however, changes the detection task dramatically: while the average treatment effect is zero, there is still a clear difference in the outcome distribution between treated and control individuals.

Figure 2a shows how each method's detection power and accuracy change as we vary each of three parameters that contribute to the strength of the treatment effect. If we compare these simulations to those above with a mean shift, TESS exhibits a consistent pattern of performance, while the performance of the competing methods is dramatically lower. The detection power results indicate that, for the competing methods, it is hard to distinguish even strong distributional changes from random chance, while the accuracy results indicate that their pinpointing of the affected subpopulation is little better than random guessing. Given that there is no observable mean shift in these simulations, these results are consistent with what we expect: TESS is designed to identify more general distributional changes, while the other methods are unable to identify distributional changes without corresponding mean shifts.

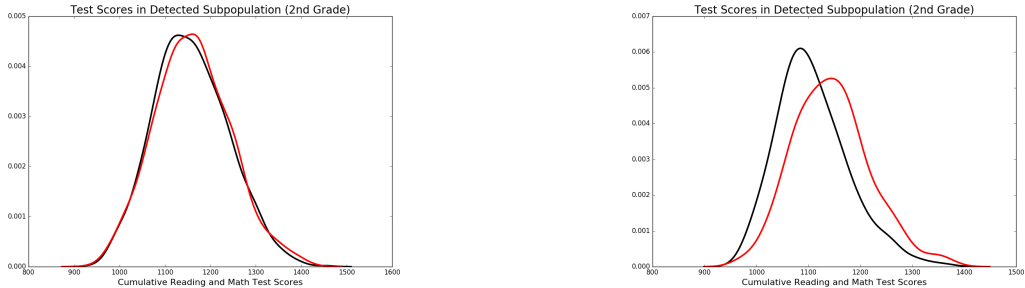
## 5.4 A Case Study on Identifying Subpopulations: Tennessee STAR

There appears to be a consensus in the literature that the presence of a teaching aide in a regular-size classroom has an insignificant effect on test scores [14, 26, 33, 42]. (One significant effect was observed in first grade, but this effect was largely considered to be a false positive.) Therefore, we want to use TESS to compare regular classrooms with an aide to regular classrooms without an aide, to determine if there appears to be a subpopulation that was significantly and positively affected by the treatment. To do so, we replicated the analysis of the internal STAR team, using TESS to extend the results, with the goal of demonstrating what the STAR team could have surmised with present-day tools for uncovering heterogeneity. We replicate the original STAR analysis from [33, 42] which includes the sum of the Stanford math and reading scores as the outcome of interest. For the data provided to TESS for detection, we combine the panel data across years and include student's grade level as a covariate. We would also like to obtain an unbiased estimate of the average treatment effect in the subpopulation identified by TESS. Therefore, we follow a cross-validation paradigm, where the entire dataset is partitioned into ten folds, and iteratively each fold is held out as a validation set (to obtain an estimate of the treatment effect) while the remaining nine folds are provided to TESS (for detection). We further partition the data into records corresponding to students observed in a regular classroom with an aide and a regular classroom without an aide, which serve as treatment and control groups respectively. In three of the ten folds, TESS identified the exact same subset which we will call the "detected subpopulation". Essentially, this detected subpopulation is composed of students in second or third grade, who attended an inner-city or urban school, receiving instruction from a teacher with 10 or more years of experience<sup>1</sup>. Therefore, it appears that the presence of an aide raised the test-scores of students exhibiting the selected covariate values described above for grade, school type, and teacher experience, in addition to any values for gender, free-lunch status, teacher ethnicity, and teacher degree. The subpopulations that were returned in each of the ten folds exhibited a large amount of agreement with the detected subpopulation: the fold subpopulations exhibited 88% agreement (on average) with the detected subpopulation on the detection status of a record. The estimated average treatment effect for this detected subpopulation, averaged across all validation folds, is approximately a 34.19 point increase in total test score (36.45 and 22.28 for second and third grades respectively).

Given this consistency across folds, we use the full data to better understand the effect in the detected subpopulation generally. Table 3 shows the evaluation of the treatment effect for all second-grade students (column 1), second-grade students in the detected subpopulation (column 2), and second-grade students in the complement of the detected subpopulation (column 3). Additionally, Figure 3 shows the kernel density plots of the cumulative scores for all second-grade students and students in the detected subpopulation respectively. Figure 3a depicts a strong similarity in the distribution of all second graders' scores with and

---

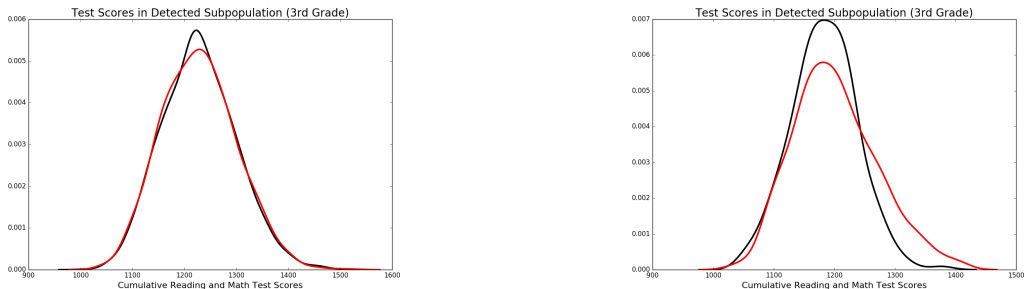
<sup>1</sup>The detected subpopulation technically excluded teacher experience between 25 and 30 years. Including this range yields qualitatively the same results and conclusions.



(a) All students in 2nd grade

(b) Detected Subpopulation in 2nd grade

Figure 3: Kernel density plots of 2nd grade test scores for treatment students (red) who were in a regular classroom with a teacher's aide and control students (black) who did not have a teacher's aide.



(a) All students in 3rd grade

(b) Detected Subpopulation in 3rd grade

Figure 4: Kernel density plots of 3rd grade test scores for treatment students (red) who were in a regular classroom with a teacher's aide and control students (black) who did not have a teacher's aide.

	All (2 <sup>nd</sup> )	Detected (2 <sup>nd</sup> )	Undetected (2 <sup>nd</sup> )	All (3 <sup>rd</sup> )	Detected (3 <sup>rd</sup> )	Undetected (3 <sup>rd</sup> )
Treatment	3.479	36.066***	1.309	-0.291	18.703***	0.1
(std. dev.)	(2.547)	(6.055)	(2.772)	(2.277)	(5.18)	(2.478)
P-value	0.172	<0.001	0.637	0.898	<0.001	0.968
Observations	4263	620	3643	4063	706	3357

Table 3: Table of estimated treatment effects on student test scores in 2nd and 3rd grade. \*\*\* indicates  $p < 0.001$ .

without a full-time aide; there is a slight difference around center of the distribution, but its magnitude is not sufficiently large to be significant, as seen by column 1 of Table 3. Conversely, Figure 3b depicts a difference in test scores for the detected subpopulation of second graders: there appears to be a clear effect of the treatment (dominated by a large mean shift), supported by column 2 of Table 3. We conduct a similar analysis with third graders, and observe similar results in Figure 4 and Table 3. However, the effect of the treatment in third grade appears to result in less of a mean shift, and is better characterized by a change in the skew (third moment) and therefore, the overall form of the distribution (Figure 4b). We note that because TESS is able to identify effects that change the distribution (and therefore higher order moments) of test scores, even if the difference in mean score between treatment and control students in third grade was smaller, TESS could potentially still identify the existence of a treatment effect.

There appears to be another consensus in the literature that small classrooms have a consistent, positive, and significant effect [14, 26, 42]; therefore, we also compare small classrooms to regular classrooms, and determine whether there appears to be a subpopulation which is the main driver of this effect. We conduct an analysis as above but with STAR data records corresponding to students observed in a small classroom (treatment group) and a regular classroom (control group). For this analysis, TESS identified the entire population, which is congruent with the previous literature's analysis of the consistent and significant average

treatment effect in each grade. This result from TESS appears to indicate that the effect of small classroom size was not limited to a specific subpopulation. For both TESS analyses, we also conducted permutation testing to compensate for multiple hypothesis testing. Based on these results, we conclude that there is a less than 0.01% chance we would obtain a subpopulation with a score as extreme under the null hypothesis.

The detected subpopulation in the classrooms with aides is not only statistically significant, but may also provide domain insight into the efficacy of full-time aides. A possible explanation for the effect we observe in the detected subpopulation is the fact that 13 schools were chosen at random to have teachers participate in an in-service training session, which the literature has also deemed ineffective [42]. More specifically, fifty-seven teachers were selected each summer from these schools to participate in a three-day in-service to help them teach more effectively in whatever class type they were assigned to; part of the instruction focused on how to work with an aide and also had the aides present. It is possible that when provided proper training, the combination of an aide and an experienced teacher can provide a significantly enhanced education environment even in the challenging teaching environments that exist in inner-city and urban schools. An additional explanation is that the educational benefits may be cumulative—i.e., in each additional year a student in this subpopulation has access to the combination of an aide and experienced teacher, the treatment effect compounds—similar to what has been demonstrated in small classrooms for the overall population [26]. However, unlike in small classrooms, for this subpopulation in regular classrooms with an aide, the effects were not large enough to be distinguishable from zero (given the much smaller sample size of the affected subpopulation and smaller treatment effect) until after two years. While a more detailed follow-up analysis of these hypotheses might reveal other causal factors at work, we believe that these results do present evidence that a treatment previously believed to be ineffective may actually have been effective for a particularly vulnerable subpopulation. Therefore, this analysis provides a sense of how TESS can be utilized as a tool for data-driven hypothesis generation in real-world policy analysis.

## 6 Conclusions

This paper has presented several contributions to the literature on statistical machine learning approaches for heterogeneous treatment effects. We proposed the Distribution Average Treatment Effect (DATE) estimand, which generalizes the focal estimands used in this literature. Moreover, as a specific example of DATE, we derived the Nonparametric Average Treatment Effect (NATE) estimand, which allows detection of treatment effects that manifest as arbitrary effects on the potential outcome distributions, rather than being limited to detection of mean shifts. Furthermore, we consider the challenge of identifying whether any subpopulation has been affected by treatment, and precisely characterizing the affected subpopulation, as opposed to the more typical problem setting of estimating individual-level treatment effects. We formalize the identification of subpopulations with significant treatment effects as an anomalous pattern detection problem, and present the Treatment Effect Subset Scan (TESS) algorithm, which serves as a computationally efficient test statistic for the maximization of our NATE estimand over all subpopulations. We demonstrate that the estimator used by TESS satisfies the linear-time subset scanning property, allowing it to be efficiently and exactly optimized over subsets of a covariate’s values, while evaluating only a linear rather than exponential number of subsets. This efficient conditional optimization step is incorporated into an iterative procedure which jointly maximizes over subsets of values for each covariate in the data: the result is a subpopulation, described as a subset of values for each covariate, which demonstrates the most evidence for a statistically significant treatment effect. In addition to its computational efficiency, we derive desirable statistical properties for the TESS estimator: bounded asymptotic probability of Type I and Type II errors, as well as providing sufficient conditions under the alternative hypothesis that will result in TESS exactly identifying the affected subpopulation. These properties apply more generally to the class of nonparametric scan statistics, upon which TESS is built; therefore, this theory also serves as a contribution to the anomalous pattern detection and scan statistics literatures.

In addition to proposing a novel algorithm with desirable properties, we provide an extensive comparison between TESS and other recently proposed statistical machine learning methods for heterogeneous treatment effects (Causal Tree, Interaction Tree, and Causal Forest) through semi-synthetic simulations. Our results

indicate that TESS consistently outperforms the other methods in its ability to identify and precisely characterize subpopulations which exhibit treatment effects. TESS significantly outperforms competing methods in the challenging scenarios where the treatment effect signal is weak (i.e., the signal magnitude is low or the affected subpopulation is small) because the subset scanning approach allows it to combine subtle signals across various dimensions of data in order to identify effects of interest. Moreover, TESS’s detection performance is consistent even when the treatment outcome distribution in the affected subpopulation has the same mean as the control outcome distribution, while the competing methods demonstrate essentially no ability to identify the affected subpopulation in the absence of a mean shift.

After demonstrating TESS’s performance through simulation, we explore the well-known Tennessee STAR experiment, searching for previously unidentified subpopulations with significant treatment effects. As a result of this analysis, TESS uncovered an intuitive subpopulation that seems to have experienced extremely significant improved test scores as a result of having a teacher’s aide in the classroom, a treatment that has consistently been considered ineffective (as measured by the average treatment effect) by the literature on the Tennessee STAR. This provides a sense of how TESS can be utilized as a tool for generating hypotheses to be further explored and tested. We do however caution researchers to view algorithms like TESS not as a replacement, but rather an assistive tool, for developing scientific and behavioral theory. Results discovered by these methods should be investigated further and evaluated to develop a deeper theoretical understanding of the phenomena they uncover. When used to this end, these tools fill a critical void: in many contexts it is rare to know *a priori* which hypotheses are relevant and supported by data, and the use of traditional methods (e.g., regression) puts the onus on the researcher to know which hypothesis to test. This process necessitates that theory comes first, and subsequent investigation is a form of confirmatory analysis. However, such a process can become an impediment to data-driven discovery: there is an increasing need for scalable methods to use (big) data to generate new hypotheses, rather than just confirming pre-existing beliefs.

In the late 1970s, John W. Tukey began to outline his vision for the future of statistics, which included a symbiotic relationship between exploratory and confirmatory data analysis. He argues these two forms of data analysis “can—and should—proceed side by side” [37] because he believed ideas “come from previous exploration more often than from lightning strokes” [38]. To this end Tukey advocates for using data to suggest hypotheses to test, or what we now call data-driven hypothesis generation. We see our work as the natural evolution of Tukey’s vision of data analysis: we develop an approach—rigorously conducted and theoretically grounded—to conduct exploratory analysis in randomized experiments, with the hope of catalyzing “lightning strokes” of discovery and the advancement of science.

## References

- [1] J. U. Adams. Genetics: Big hopes for big data. *Nature*, 527:S108–S109, Nov 2015.
- [2] A. Alyass, M. Turcotte, and D. Meyre. From big data analysis to personalized medicine for all: challenges and opportunities. *BMC Medical Genomics*, 8(1):613, Jun 2015.
- [3] M. L. Anderson. Multiple inference and gender differences in the effects of early intervention: A reevaluation of the Abecedarian, Perry preschool, and Early Training projects. *Journal of the American Statistical Association*, 103:1481–1495, Dec 2008.
- [4] J. D. Angrist and J.-S. Pischke. *Mostly Harmless Econometrics: An Empiricist’s Companion*. Princeton University Press, Dec 2008.
- [5] F. J. Anscombe. Graphs in statistical analysis. *The American Statistician*, 27(1):17, Feb 1973.
- [6] S. F. Assmann, S. J. Pocock, L. E. Enos, and L. E. Kasten. Subgroup analysis and other (mis)uses of baseline data in clinical trials. *The Lancet*, 355:1064–1069, 2000.
- [7] S. Athey and G. Imbens. Recursive partitioning for heterogeneous causal effects. *Proceedings of the National Academy of Sciences*, 113(27):7353–7360, Jul 2016.

- [8] W. S. Barnett. Benefit-cost analysis of the Perry preschool program and its policy implications. *Educational evaluation and policy analysis*, 7(4):333–342, Jan 1985.
- [9] R. H. Berk and D. H. Jones. Goodness-of-fit test statistics that dominate the Kolmogorov statistics. *Zeitschrift für Wahrscheinlichkeitstheorie und Verwandte Gebiete*, 47:47–59, 1979.
- [10] J. N. Cohn, D. G. Archibald, S. Ziesche, and Others. Effect of vasodilator therapy on mortality in chronic congestive heart failure. *New England Journal of Medicine*, 314(24):1547–1552, Jun 1986.
- [11] J. N. Cohn, G. Johnson, S. Ziesche, and Others. A comparison of enalapril with hydralazine-isosorbide dinitrate in the treatment of chronic congestive heart failure. *New England Journal of Medicine*, 325(5):303–310, Aug 1991.
- [12] E. Duflo. Field experiments in development economics. In R. Blundell, W. Newey, and T. Persson, editors, *Advances in Economics and Econometrics: Theory and Applications, Ninth World Congress*, volume 2, pages 322–348. 2006.
- [13] A. Dvoretzky, J. Kiefer, and J. Wolfowitz. Asymptotic minimax character of the sample distribution function and of the classical multinomial estimator. *The annals of mathematical statistics*, 27(3):642–669, Sep 1956.
- [14] J. Folger and C. Breda. Evidence from project STAR about class size and student achievement. *Peabody Journal of Education*, 67(1):17–33, Sep 1989.
- [15] U. Food and D. Administration. FDA approves BiDil heart failure drug for black patients. Press Release, June 2005. <http://www.fda.gov/NewsEvents/Newsroom/PressAnnouncements/2005/ucm108445.htm>.
- [16] J. H. Friedman. Multivariate adaptive regression splines. *Annals of Statistics*, 19(1):1–67, Mar 1991.
- [17] P. Gaensler and J. A. Wellner. *Glivenko–Cantelli Theorems*. John Wiley & Sons, Inc., Hoboken, NJ, USA, Jul 2004.
- [18] D. P. Green and H. L. Kern. Modeling heterogeneous treatment effects in survey experiments with Bayesian additive regression trees. *Public Opinion Quarterly*, 76(3):491–511, Sep 2012.
- [19] J. Grimmer, S. Messing, and S. J. Westwood. Estimating heterogeneous treatment effects and the effects of heterogeneous treatments with ensemble methods. *Political Analysis*, Conditional Acceptance, 2017.
- [20] T. Hastie, R. Tibshirani, and J. Friedman. *The Elements of Statistical Learning*. Springer Series in Statistics. Springer New York, New York, NY, 2009.
- [21] K. Imai and M. Ratkovic. Estimating treatment effect heterogeneity in randomized program evaluation. *The Annals of Applied Statistics*, 7(1):443–470, Mar 2013.
- [22] G. W. Imbens and J. M. Wooldridge. Recent developments in the econometrics of program evaluation. *Journal of Economic Literature*, 47(1):5–86, Mar 2009.
- [23] L. Jager and J. A. Wellner. Goodness-of-fit tests via phi-divergences. *The Annals of Statistics*, 35(5):2018–2053, Oct 2007.
- [24] B. Kasenda, S. Schandelmaier, and Sun, Xin et al. Subgroup analyses in randomised controlled trials: cohort study on trial protocols and journal publications. *BMJ*, 349, Jul 2014.
- [25] R. Kohavi, A. Deng, B. Frasca, T. Walker, Y. Xu, and N. Pohlmann. Online controlled experiments at large scale. In *Proceedings of the 19th ACM SIGKDD International Conference on Knowledge Discovery and Data Mining*, New York, NY, USA, 2013.

- [26] A. B. Krueger. Experimental estimates of education production functions. *The Quarterly Journal of Economics*, 114(2):497–532, May 1999.
- [27] S. W. Lagakos. The challenge of subgroup analyses — reporting without distorting. *New England Journal of Medicine*, 354(16):1667–1669, Apr 2006.
- [28] E. McFowland III, S. D. Speakman, and D. B. Neill. Fast generalized subset scan for anomalous pattern detection. *The Journal of Machine Learning Research*, 14(1):1533–1561, Jun 2013.
- [29] D. B. Neill. Fast subset scan for spatial pattern detection. *Journal of the Royal Statistical Society (Series B: Statistical Methodology)*, 74(2):337–360, 2012.
- [30] D. W. Nickerson and T. Rogers. Political campaigns and big data. *Journal of Economic Perspectives*, 28(2):51–74, May 2014.
- [31] B. Nye, L. V. Hedges, and S. Konstantopoulos. The effects of small classes on academic achievement: The results of the Tennessee class size experiment. *American Educational Research Journal*, 37(1):123–151, 2000.
- [32] L. J. Schweinhart, H. V. Barnes, and D. P. Weikart. Significant benefits: The High/Scope Perry preschool study through age 27. Technical Report 10, High/Scope Educational Research Foundation, 1993.
- [33] J. Stock and M. Watson. *Introduction to Econometrics 2nd edition*. Pearson, 2007.
- [34] X. Su, C.-L. Tsai, H. Wang, D. M. Nickerson, and B. Li. Subgroup analysis via recursive partitioning. *Journal of Machine Learning Research*, 10:141–158, Dec 2009.
- [35] L. Tian, A. A. Alizadeh, A. J. Gentles, and R. Tibshirani. A simple method for estimating interactions between a treatment and a large number of covariates. *Journal of the American Statistical Association*, 109(508):1517–1532, Dec 2014.
- [36] R. Tibshirani. Regression shrinkage and selection via the lasso. *Journal of the Royal Statistical Society, Series B*, 58:267–288, 1996.
- [37] J. W. Tukey. *Exploratory Data Analysis*. Addison-Wesley Publishing Company, 1977.
- [38] J. W. Tukey. We need both exploratory and confirmatory. *The American Statistician*, 34(1), 1980.
- [39] H. R. Varian. Big data: New tricks for econometrics. *Journal of Economic Perspectives*, 28(2):3–28, May 2014.
- [40] S. Wager and S. Athey. Estimation and inference of heterogeneous treatment effects using random forests. *Journal of the American Statistical Association*, 2018.
- [41] H. I. Weisberg and V. P. Pontes. Post hoc subgroups in clinical trials: Anathema or analytics? *Clinical trials*, 12(4):357–364, Aug 2015.
- [42] E. R. Word, J. Johnston, H. P. Bain, and Others. The state of Tennessee’s Student/Teacher Achievement Ratio (STAR) project: Technical report 19851990. *Nashville: Tennessee State Department of Education*, 1990.

## SUPPLEMENTARY MATERIAL

To begin we revisit the general form of the score function—or equivalently the treatment effect test statistic—that we refer to as the nonparametric scan statistic. Additionally, we establish equivalences, as different forms will lend themselves to various proof strategies we implement later.

$$\begin{aligned}
\max_S F(S) &= \max_{S,\alpha} F_\alpha(S) &= \max_{S,\alpha,\beta} F_{\alpha,\beta}(S) \\
&= \max_{S,\alpha} \phi(\alpha, N_\alpha(S), N(S)) = \max_{S,\alpha,\beta} \sum_{s_i \in S} \omega(\alpha, \beta, n_\alpha(s_i), n(s_i)).
\end{aligned} \tag{13}$$

First, we demonstrate that our empirical distribution functions from the control and treatment groups are unbiased estimators under this assumption of unconfoundedness.

**Lemma 1.** *If  $Y_i(0), Y_i(1) \perp\!\!\!\perp W_i | X_i$ , then  $\hat{F}_{Y^C|X=x}$  and  $\hat{F}_{Y^T|X=x}$  are unbiased estimators of  $F_{Y(0)|X=x}$  and  $F_{Y(1)|X=x}$  respectively.*

*Proof.*

$$\begin{aligned}
\mathbb{E} \left[ \hat{F}_{Y^C|X=x}(y) \right] &= \mathbb{E}_{Y|X=x} \left[ \frac{\sum_{U_i:X_i=x} \mathbb{1}\{W_i=0\} \mathbb{1}\{Y_i^{\text{obs}} \leq y\}}{\sum_{U_i:X_i=x} \mathbb{1}\{W_i=0\}} \right] \\
&= \mathbb{E}_{W|X=x} \left[ \mathbb{E}_{Y|W,X=x} \left[ \frac{\sum_{U_i:X_i=x} \mathbb{1}\{W_i=0\} \mathbb{1}\{Y_i^{\text{obs}} \leq y\}}{\sum_{U_i:X_i=x} \mathbb{1}\{W_i=0\}} \right] \right] \\
&= \mathbb{E}_{W|X=x} \left[ \frac{\sum_{U_i:X_i=x} \mathbb{1}\{W_i=0\} \mathbb{E}_{Y|W_i=0,X_i=x} [\mathbb{1}\{Y_i(0) \leq y\}]}{\sum_{U_i:X_i=x} \mathbb{1}\{W_i=0\}} \right] \\
&= \mathbb{E}_{W|X=x} \left[ \frac{\sum_{U_i:X_i=x} \mathbb{1}\{W_i=0\} \mathbb{E}_{Y|X_i=x} [\mathbb{1}\{Y_i(0) \leq y\}]}{\sum_{U_i:X_i=x} \mathbb{1}\{W_i=0\}} \right] \\
&= \mathbb{E}_{W|X=x} \left[ \mathbb{E}_{Y|X_i=x} [\mathbb{1}\{Y_i(0) \leq y\}] \frac{\sum_{U_i:X_i=x} \mathbb{1}\{W_i=0\}}{\sum_{U_i:X_i=x} \mathbb{1}\{W_i=0\}} \right] \\
&= \mathbb{E}_{W|X=x} [\mathbb{E}_{Y|X_i=x} [\mathbb{1}\{Y_i(0) \leq y\}]] \\
&= \mathbb{E}_{Y|X_i=x} [\mathbb{1}\{Y_i(0) \leq y\}] \\
&= F_{Y(0)|X=x}(y).
\end{aligned}$$

A similar argument shows that  $\mathbb{E} \left[ \hat{F}_{Y^T|X=x}(y) \right] = F_{Y(1)|X=x}(y)$ , assuming that unconfoundedness holds and thus the substitution  $\mathbb{E}_{Y|W_i=1,X_i=x} [\mathbb{1}\{Y_i(1) \leq y\}] = \mathbb{E}_{Y|X_i=x} [\mathbb{1}\{Y_i(1) \leq y\}]$  can be made.  $\square$

**Corollary 1.** *As a direct consequence of  $\mathbb{E} \left[ \hat{F}_{Y^C|X=x}(y) \right] = F_{Y(0)|X=x}(y)$ , we also have that  $\mathbb{E} \left[ \hat{F}_{Y^C|X=x}(y) \right]$  is strongly consistent,  $\|\hat{F}_{Y^C|X=x} - F_{Y(0)|X=x}\|_\infty \xrightarrow{\text{a.s.}} 0$ . Furthermore, the rate of convergence is exponential in sample size,  $P \left( \|\hat{F}_{Y^C|X=x} - F_{Y(0)|X=x}\|_\infty > \epsilon \right) \leq 2e^{-2n_{0,x}\epsilon^2}$   $\epsilon > 0$ , where  $n_{0,x}$  is the number of control units with  $X_i = x$ . Again similar arguments apply for  $\hat{F}_{Y^T|X=x}(y)$ .*

Given these properties of the empirical conditional distribution functions, we can now turn our attention to the score function. More specifically, we provide evidence for the expected value of  $N_\alpha(S)$  under  $H_0$ :

**Lemma 2.** *Under  $H_0$ ,  $E[N_\alpha(S)] = \alpha N(S)$ .*

*Proof.*

$$\begin{aligned}
E[N_\alpha(S)] &= E\left[\sum_{p_t \in C(S)} n_\alpha(p_t)\right] \\
&= \sum_{p_t \in C(S)} E[n_\alpha(p_t)] \\
&= \sum_{p_t \in C(S)} \alpha \\
&= \alpha N(S).
\end{aligned}$$

□

## TESS Computational Theory

For consistency with previous work, we will use the established notation—e.g.,  $F$ ,  $F_\alpha$ , and  $\phi$ —when describing the computational theory, as this theory is generally applicable to anomalous pattern detection. Consistent with [28], we also assume that for a fixed value of  $\alpha$  the following conditions are satisfied:

- (A1)  $\phi$  is monotonically **increasing** w.r.t.  $N_\alpha$ .
- (A2)  $\phi$  is monotonically **decreasing** w.r.t.  $N$ .
- (A3)  $\phi$  is **convex** w.r.t.  $N_\alpha$  and  $N$ .

These assumptions are intuitive because the ratio of observed to expected number of significant  $p$ -values  $\frac{N_\alpha}{\alpha N}$  increases with the numerator (A1) and decreases with the denominator (A2). Also, a fixed ratio of observed to expected should be more significant when the observed and expected counts are large (A3). Our objective is to show that satisfying these intuitive assumptions allows a function to be efficiently optimized. In §3.5 we have already introduced the Berk-Jones statistic and the Normal Approximation. Below we will introduce a number of the other well-known supremum goodness-of-fit statistics, demonstrate that these statistics satisfy these assumptions, and therefore can be efficiently maximized by the nonparametric scan statistic.

## Proof of TESS Efficient Scanning

According to [29], for a given set of data elements  $D = \{R_1 \dots R_n\}$ , a score function  $F(S)$  mapping  $S \subseteq D$  to a real number, and a priority function  $G(R_i)$  mapping a single data element  $R_i \in D$  to a real number, the LTSS property guarantees that the only subsets with the potential to be optimal are those consisting of the top- $k$  highest priority records  $\{R_{(1)} \dots R_{(k)}\}$ , for some  $k$  between 1 and  $n$ . More formally, we restate that theorem as

**Theorem 1.** *Let  $F(S) = F(X, Y)$  be a function of two additive sufficient statistics of subset  $S$ ,  $X(S) = \sum_{R_i \in S} x_i$  and  $Y(S) = \sum_{R_i \in S} y_i$ , where  $x_i$  and  $y_i$  depend only on record  $R_i$ . Assume that  $F(S)$  is monotonically increasing with  $X(S)$ , that all  $y_i$  values are positive, and that  $F(X, Y)$  is convex. Then  $F(S)$  satisfies the LTSS property with priority function  $G(R_i) = \frac{x_i}{y_i}$ .*

**Corollary 2.** *We consider the general class of nonparametric scan statistics as defined in (13), where the significance level  $\alpha$  is allowed to vary from zero to some constant  $\alpha_{max}$ . For a given value of  $\alpha$  and  $v^{-j} = \{v^1, \dots, v^{j-1}, v^{j+1}, \dots, v^d\}$  under consideration, we demonstrate that  $F_\alpha(S)$  can be efficiently maximized over all subpopulations  $S = v^j \times v^{-j}$ , for  $v^j \subseteq V^j$ . First, we note that number of  $p$ -value ranges in every  $v^j$  is positive: we only consider the values of a covariate that are expressed by some treatment unit, as there can be no treatment effect to observe if there are not units with particular characteristics. Thus we have*

$$F_\alpha(S) = \phi(\alpha, N_\alpha(v^j), N(v^j)), \quad (14)$$

where the additive sufficient statistic  $N_\alpha(v^j)$  is defined as follows:

$$N_\alpha(v^j) = \sum_{p_t \in C(v^j \times v^{-j})} n_\alpha(p_t),$$

and the additive sufficient statistic  $N(v^j)$  is defined as follows:

$$N(v^j) = \sum_{p_t \in C(v^j \times v^{-j})} 1.$$

Since the nonparametric scan statistic is defined to be monotonically increasing with  $N_\alpha$  (A1), monotonically decreasing with  $N$  (A2), and convex (A3), we know that  $F_\alpha(S)$  satisfies the LTSS property with priority function over the values of mode (covariate)  $j$  ( $v_m^j \in V^j$ )

$$G_\alpha(v_m^j) = \frac{\sum_{p_t \in C(v_m^j \times v^{-j})} n_\alpha(p_t)}{\sum_{p_t \in C(v_m^j \times v^{-j})} 1}. \quad (15)$$

Therefore the LTSS property holds for each value of  $\alpha$ , enabling each  $F_\alpha(S)$  to be efficiently maximized over subsets of values for the  $j^{\text{th}}$  mode of the tensor, given values for the other  $d - 1$  modes.

Additionally, [28] demonstrates that only small set of  $\alpha$  levels must be examined in order to optimize the nonparametric scan statistic over all values of  $\alpha$ , for  $0 < \alpha \leq \alpha_{\max} \leq 1$ . More precisely, only the maximum value  $p_{\max}(p_t)$  of each  $p$ -value range  $p_t \leq \alpha_{\max}$  in the subpopulation  $S$  must be considered as a possible value of  $\alpha$ . If  $U(S, \alpha_{\max})$  is the set of unique  $\alpha$  values to be considered for subpopulation  $S$ —for  $|U(S, \alpha_{\max})| \leq n_t$ , recalling that  $n_t$  is the total number of treatment units—then

$$\begin{aligned} \max_S F(S) &= \max_\alpha \max_S F_\alpha(S) \\ &= \max_{\alpha \in U(S, \alpha_{\max})} \max_S F_\alpha(S) \end{aligned} \quad (16)$$

can be efficiently and exactly computed over all subsets  $S = v^j \times v^{-j}$ , where  $v^j \subseteq V^j$ , for a given subset of values for each of the other modes  $v^{-j}$ . To do so, consider the set of distinct  $\alpha$  values  $U = U(V^j \times v^{-j}, \alpha_{\max})$ . For each  $\alpha \in U$ , we employ the same logic as described in Corollary (2) to optimize  $F_\alpha(S)$ : compute the priority  $G_\alpha(v_m^j)$  for each value ( $v_m^j \in V^j$ ) as in (15), sort the values from highest to lowest priority, and evaluate subsets  $S = \{v_{(1)}^j \dots v_{(k)}^j\} \times v^{-j}$  consisting of the top- $k$  highest priority values, for  $k = 1 \dots |V^j|$ .

TESS then iterates over modes of the tensor, using the efficient optimization steps described above to optimize each mode:

$$v^j = \arg \max_{v^j \subseteq V^j} F(v^j \times v^{-j}) \quad j = 1 \dots d, \quad (17)$$

continuing to compute (17) until convergence. A single iteration (optimization of mode  $j$  of the tensor) has a complexity of  $O(|U|(n_t + |V^j| \log |V^j|))$ , where  $U = U(V^j \times v^{-j}, \alpha_{\max})$ ; the  $n_t$  term, the number of (unique) treatment units, results from collecting the  $p$ -value ranges for all units in  $C(V^j \times v^{-j})$  over our sparse tensor; and  $O(|V^j| \log |V^j|)$  is required to sort the values of tensor mode  $j$ . Therefore a step in the procedure (a sequence of  $d$  iterations over all modes of the tensor) has complexity  $O(|U|d(n_t + |V| \log |V|))$ , where  $|U|$  and  $|V|$  are the average numbers of  $\alpha$  thresholds considered and covariate arity, respectively. Thus the TESS search procedure has a total complexity of  $O(IZ|U|d(n_t + |V| \log |V|))$ , where  $I$  is the number of random restarts and  $Z$  is the average number of iterations required for convergence.

## TESS Algorithm

Inputs: randomized experiment dataset,  $\alpha_{\max}$ , number of iterations  $I$ .

1. Separate randomized experiment dataset into treatment and control groups.

2. For each unique covariate profile  $x_u$  in the treatment group:
  - (a) Estimate  $\hat{F}_{Y^C|X=x_u}$  from the outcomes of the units in the control group that share profile  $x_u$ .
  - (b) Compute the  $p$ -value range  $p_t = [p_{\min}(p_{ij}), p_{\max}(p_{ij})]$  for each treatment unit  $t$  with profile  $x_u$  from  $\hat{F}_{Y^C|X=x_u}$ .
3. Iterate the following steps  $I$  times. Record the maximum value  $F^*$  of  $F(S)$ , and the corresponding subsets of values for each mode  $\{v^{1*}, \dots, v^{d*}\}$  over all such iterations:
  - (a) For each of the  $d$  modes:
    - i. Initialize  $v^j \leftarrow$  random subset of values  $V^j$ .
  - (b) Repeat until convergence:
    - i. For each of the  $d$  modes:
      - A. Maximize  $F(S) = \max_{\alpha \leq \alpha_{\max}} F_{\alpha}(v^j \times v^{-j})$  over subsets of values for  $j^{th}$  mode  $v^j \subseteq V^j$ , for the current subset of values of the other  $d-1$  modes  $(v^{-j})$ , and set  $v^j \leftarrow \arg \max_{v^j \subseteq V^j} F(v^j \times v^{-j})$ .
4. Output  $S^* = \{v^{1*}, \dots, v^{d*}\}$ .

## Score Functions

In §3.5 we introduced two score functions: Berk-Jones  $F_{\alpha}^{BJ}(S) = N(S)Div_{KL}\left(\frac{N_{\alpha}(S)}{N(S)}, \alpha\right)$ , where  $Div_{KL}$  is the Kullback-Liebler divergence, and the Normal Approximation  $F_{\alpha}^{NA}(S) = N(S)Div_{\frac{1}{2}\chi^2}\left(\frac{N_{\alpha}(S)}{N(S)}, \alpha\right) = \frac{(N_{\alpha}(S) - N(S)\alpha)^2}{2N(S)\alpha(1-\alpha)}$ . There are a collection of well-known supremum goodness-of-fit statistics used in the literature (all of which are described in [23]) that are each a transformation of  $F_{\alpha}^{NA}(S)$ : the Kolmogorov-Smirnov statistic

$$\begin{aligned} F^{KS}(S) &= \max_{\alpha} F_{\alpha}^{KS}(S) \\ &= \max_{\alpha} \frac{(N_{\alpha}(S) - N(S)\alpha)^2}{\sqrt{N(S)}} \\ &= \max_{\alpha} \sqrt{2\alpha(1-\alpha)F_{\alpha}^{NA}(S)}, \end{aligned}$$

the Cramer-von Mises statistic

$$\begin{aligned} F^{CV}(S) &= \max_{\alpha} F_{\alpha}^{CV}(S) \\ &= \max_{\alpha} \frac{(N_{\alpha}(S) - N(S)\alpha)^2}{N(S)} \\ &= \max_{\alpha} 2\alpha(1-\alpha)F_{\alpha}^{NA}(S), \end{aligned}$$

the Higher-Criticism statistic

$$\begin{aligned} F^{HC}(S) &= \max_{\alpha} F_{\alpha}^{HC}(S) \\ &= \max_{\alpha} \frac{(N_{\alpha}(S) - N(S)\alpha)^2}{\sqrt{N(S)\alpha(1-\alpha)}} \\ &= \max_{\alpha} \sqrt{2F_{\alpha}^{NA}(S)}, \end{aligned}$$

and the Anderson-Darling statistic

$$\begin{aligned}
F^{AD}(S) &= \max_{\alpha} F_{\alpha}^{AD}(S) \\
&= \max_{\alpha} \frac{(N_{\alpha}(S) - N(S)\alpha)^2}{N(S)\alpha(1-\alpha)} \\
&= \max_{\alpha} 2F_{\alpha}^{NA}(S).
\end{aligned}$$

As a result of this connection between  $F^{NA}$  and these other statistics, we have the following:

**Lemma 3.** *If  $S$  maximizes  $F_{\alpha}^{NA}(S)$ , then it maximizes  $F_{\alpha}^{KS}(S)$ ,  $F_{\alpha}^{CV}(S)$ ,  $F_{\alpha}^{HC}(S)$  and  $F_{\alpha}^{AD}(S)$ .*

*Proof.* First, we note that  $T(F_{\alpha}^{NA})$ , where  $T(x) = (bx)^a$ , for  $b \in \{1, 2, 2\alpha(1-\alpha)\}$  and  $a \in \{1, \frac{1}{2}\}$  is a monotonically increasing transformation. Therefore,  $\arg \max_{\alpha} F_{\alpha}^{NA}(S) = \arg \max_{\alpha} T(F_{\alpha}^{NA}(S))$ , because  $\arg \max$  is invariant to monotone transformations.  $\square$

## Statistical Properties

We will now proceed to demonstrate desirable statistical properties of  $F^{BJ}(S)$  and  $F^{NA}(S)$  directly; these properties will also extend to the other statistics described above because of their close relationship to  $F^{NA}(S)$ . More specifically, we now aim to demonstrate that using  $F(S)$  we can appropriately (fail to) reject  $H_0$  with high probability. We will introduce some notation that will be used in the analysis below.

### Notation

$S^T$ : the truly affected (rectangular (8)) subset.

$S^*$ : the most anomalous (rectangular) subset,  $\arg \max_{S \in R} F(S)$ , where  $R$  is the space of all rectangular subsets.

$\alpha^*$ : the  $\alpha$  at which  $S^*$  is most anomalous,  $\arg \max_{\alpha} F_{\alpha}(S^*)$ .

$S_u^*$ : the most anomalous unconstrained subset,  $\arg \max_{S \in R} F(S)$ .

$\alpha_u^*$ : the  $\alpha$  at which  $S_u^*$  is most anomalous,  $\arg \max_{\alpha} F_{\alpha}(S_u^*)$ .

$M$ : the number of non-empty cells in the tensor—i.e., the number of unique covariate profiles  $x_t$  in the treatment group that also exist in the control group.

$k$ : the proportion of non-empty cells that are affected under  $H_1(S^T)$ .

$\beta(\alpha)$ :  $P(p_t \leq \alpha | H_1(S^T)) \quad \forall p_t \in S^T$ , that is,  $p_t$  are the p-value ranges of all the cells  $S^T$ .

$h(M)$ : a critical value of  $\max_{S \in R} F(S)$  for a given  $M$ .

$\phi$ : Probability density function of standard normal.

$\Phi$ : Cumulative distribution function of standard normal.

The results derived in this section assume  $n(s) \geq n \quad \forall s \in D$ , i.e., that each non-empty cell (unique covariate profile) in the data has at least  $n$  data points. More specifically, we would like to show in the limit:

$$\begin{aligned}
P_{H_0} \left( \max_{S \in R} F(S) > h(M) \right) &\rightarrow 0, \\
P_{H_1} \left( \max_{S \in R} F(S) > h(M) \right) &\rightarrow 1.
\end{aligned}$$

The first result we show is that in the limit  $F^{BJ}$  is well approximated by  $F^{NA}$ , which will then allow us to focus the remainder of our results on  $F^{NA}$  specifically.

**Lemma 4.**  $F^{BJ}(S) \asymp F^{NA}(S)$  as  $n \rightarrow \infty$ .

*Proof.* Recall that  $K(x, y) = \text{Div}_{KL}(x, y) = x \log \frac{x}{y} + (1 - x) \log \frac{1-x}{1-y}$ , and by expanding  $K(x, y)$  through a Taylor series, we have

$$\begin{aligned} K(x, y) &= K(y, y) + \frac{\partial K(x, y)}{\partial x} \Big|_{x=y} (x - y) + \frac{\partial^2 K(x, y)}{\partial^2 x} \Big|_{x=y} \frac{(x - y)^2}{2} \\ &= 0 + 0 + \frac{(x - y)^2}{2y'(1 - y')} \end{aligned}$$

for some  $y'$  such that  $|y' - x| \leq |y - x|$ . Therefore,

$$\begin{aligned} F^{BJ}(S) &= \max_{\alpha} N(S) K\left(\frac{N_{\alpha}(S)}{N(S)}, \alpha\right) \\ &= \max_{\alpha} N(S) \frac{\left(\frac{N_{\alpha}(S)}{N(S)} - \alpha\right)^2}{2\alpha'(1 - \alpha')} \quad \left(\text{where } \left|\alpha' - \frac{N_{\alpha}(S)}{N(S)}\right| \leq \left|\alpha - \frac{N_{\alpha}(S)}{N(S)}\right|\right) \\ &\leq \max_{\alpha} N(S) \left[ \frac{\left(\frac{N_{\alpha}(S)}{N(S)} - \alpha\right)^2}{2\alpha(1 - \alpha)} \vee \frac{\left(\frac{N_{\alpha}(S)}{N(S)} - \alpha\right)^2}{2\frac{N_{\alpha}(S)}{N(S)}\left(1 - \frac{N_{\alpha}(S)}{N(S)}\right)} \right] \\ &\geq \max_{\alpha} N(S) \left[ \frac{\left(\frac{N_{\alpha}(S)}{N(S)} - \alpha\right)^2}{2\alpha(1 - \alpha)} \wedge \frac{\left(\frac{N_{\alpha}(S)}{N(S)} - \alpha\right)^2}{2\frac{N_{\alpha}(S)}{N(S)}\left(1 - \frac{N_{\alpha}(S)}{N(S)}\right)} \right]. \end{aligned}$$

Furthermore, under  $H_0$ ,  $\frac{N_{\alpha}(S)}{N(S)} \xrightarrow{a.s.} \alpha \implies \alpha' \xrightarrow{a.s.} \alpha$ , which by the continuous mapping theorem results in

$$\begin{aligned} F^{BJ}(S) &\xrightarrow{a.s.} \max_{\alpha} N(S) \frac{\left(\frac{N_{\alpha}(S)}{N(S)} - \alpha\right)^2}{2\alpha(1 - \alpha)} \\ &= F^{NA}(S). \end{aligned}$$

However, under  $H_1(S^T)$ ,  $\frac{N_{\alpha}(S)}{N(S)} \xrightarrow{a.s.} \beta(\alpha)$ , therefore asymptotically for  $F^{BJ}(S)$  we have,

$$\begin{aligned} \max_{\alpha} N(S) \frac{\left(\frac{N_{\alpha}(S)}{N(S)} - \alpha\right)^2}{2\alpha(1 - \alpha)} \left(1 \wedge \frac{\alpha(1 - \alpha)}{\beta(\alpha)(1 - \beta(\alpha))}\right) &\leq F^{BJ}(S) \\ &\leq \max_{\alpha} N(S) \frac{\left(\frac{N_{\alpha}(S)}{N(S)} - \alpha\right)^2}{2\alpha(1 - \alpha)} \left(1 \vee \frac{\alpha(1 - \alpha)}{\beta(\alpha)(1 - \beta(\alpha))}\right) \end{aligned}$$

Therefore, we can see that  $F^{BJ}(S)$  is bounded above and below by either  $F^{NA}(S)$  or a constant times  $F^{NA}(S)$ .  $\square$

Now, we will show that when the null hypothesis is true—i.e., the treatment does not have an effect—in the limit the score of the most anomalous subset is linear in  $M$ .

**Lemma 5.** *Under  $H_0$ ,  $F^{NA}(S_u^*) \xrightarrow{p} \max_Z \frac{M\phi(Z)^2}{2(1 - \Phi(Z))} \approx 0.202 M$ , where  $Z \sim N(0, 1)$ .*

*Proof.* From Theorem 1 we know that if  $\{s_{(1)}, \dots, s_{(M)}\}$  are  $M$  data elements—i.e., cells in the tensor or unique covariate profiles in the data—sorted according to priority  $\frac{n_{\alpha}(s)}{n(s)}$ , where  $s_{(k)}$  has the  $k^{th}$  highest

priority, then

$$\begin{aligned} S_u^* &= \{s_{(1)}, \dots, s_{(k)}\}_{k \in [1, M]} \\ &= \left\{ s_i \left| \frac{n_\alpha(s_i)}{n(s_i)} > t(\alpha) \right. \right\}. \end{aligned}$$

Thus it follows that  $|S| \sim \text{Bin}\left(M, P(\text{Bin}(n, \alpha) > t(\alpha)n)\right)$ ,  $\mathbb{E}_{H_0}[N(S_u^*)] = MnP(\text{Bin}(n, \alpha) > t(\alpha)n)$ , and  $\mathbb{E}_{H_0}[N_\alpha(S_u^*)] = MP(\text{Bin}(n, \alpha) \geq t(\alpha)n)\mathbb{E}[X \sim \text{Bin}(n, \alpha) | X \geq t(\alpha)n]$ . Furthermore, this implies,

$$\begin{aligned} \frac{N_\alpha(S_u^*)}{N(S_u^*)} &\xrightarrow{a.s.} \mathbb{E}\left[\frac{n_\alpha(s)}{n} \left| \frac{n_\alpha}{n} > t(\alpha)\right.\right] \\ &= \mathbb{E}\left[\frac{X \sim \text{Bin}(n, \alpha)}{n} \left| \frac{X}{n} > t(\alpha)\right.\right] \\ &\xrightarrow{d} \mathbb{E}\left[\frac{X \sim N(n\alpha, n\alpha(1-\alpha))}{n} \left| \frac{\sqrt{n}(\frac{X}{n} - \alpha)}{\sqrt{\alpha(1-\alpha)}} > Z^t(\alpha)\right.\right] \quad \left(\text{with } Z^t(\alpha) = \frac{\sqrt{n}(t(\alpha) - \alpha)}{\sqrt{\alpha(1-\alpha)}}\right) \\ &= \frac{n\alpha + \sqrt{n\alpha(1-\alpha)} \frac{\phi(Z^t(\alpha))}{(1-\Phi(Z^t(\alpha)))}}{n}. \end{aligned} \tag{18}$$

Using the definition of  $F^{NA}(S_u^*)$  we have

$$\begin{aligned} F^{NA}(S_u^*) &= \max_{\alpha} F_\alpha^{NA}(S_u^*) \\ &= \max_{\alpha} \left( \frac{N_\alpha(S_u^*)}{N(S_u^*)} - \alpha \right)^2 \frac{N(S_u^*)}{2\alpha(1-\alpha)} \\ &\xrightarrow{p} \max_{\alpha} \left( \frac{\sqrt{n\alpha(1-\alpha)} \frac{\phi(Z^t(\alpha))}{(1-\Phi(Z^t(\alpha)))}}{n} \right)^2 \frac{Mn(1-\Phi(Z^t(\alpha)))}{2\alpha(1-\alpha)} \\ &= \max_{\alpha} \frac{M\phi(Z^t(\alpha))^2}{2(1-\Phi(Z^t(\alpha)))} \approx 0.202 M, \end{aligned} \tag{19}$$

where (19) is a result of the continuous mapping theorem and (18). Furthermore, the convergence in probability of (19) is a result of the convergence in distribution to a constant.  $\square$

Now, we are able to show that the Type I error of a level- $\alpha$  test based on  $F(S)$  can be controlled in the limit.

**Theorem 2.** *Let  $n(x_t) \geq n \ \forall x_t \in D$ , i.e., assume that each of the  $M$ -many unique covariate profiles in the data (or cells in the tensor) that are non-empty in both treatment and control, has at least  $n$  data points. Additionally, assume that  $Mn \rightarrow \infty$ , then for some test level  $\gamma \in (0, 1)$  and sequence of critical values  $h(M)$ ,*

$$P_{H_0} \left( \max_{S \in R} F(S) > h(M) \right) \rightarrow 0.$$

*Proof.* First, we note that under  $H_0$

$$F(S^*) \leq F(S_u^*),$$

because the detected subset  $S^*$  is the arg max over all rectangular subsets (as defined in (8)), while  $S_u^*$  is the arg max over all subsets. We now consider the score function  $F^{NA}$  and the critical value  $h(M) =$

$$\max_{\alpha} \frac{M\phi(Z^t(\alpha))^2}{(1-\Phi(Z^t(\alpha)))} + \epsilon, \text{ for any } \epsilon > 0.$$

$$\begin{aligned}
P_{H_0}(\text{Reject } H_0) &= P_{H_0}(F^{NA}(S^*) > h(M)) \\
&= P_{H_0}\left(F^{NA}(S^*) > \max_{\alpha} \frac{M\phi(Z^t(\alpha))^2}{(1-\Phi(Z^t(\alpha)))} + \epsilon\right) \\
&\leq P_{H_0}\left(F^{NA}(S_u^*) > \max_{\alpha} \frac{M\phi(Z^t(\alpha))^2}{(1-\Phi(Z^t(\alpha)))} + \epsilon\right) \\
&= P_{H_0}\left(F^{NA}(S_u^*) - \max_{\alpha} \frac{M\phi(Z^t(\alpha))^2}{(1-\Phi(Z^t(\alpha)))} > \epsilon\right) \\
&\leq P_{H_0}\left(\left|F^{NA}(S_u^*) - \max_{\alpha} \frac{M\phi(Z^t(\alpha))^2}{(1-\Phi(Z^t(\alpha)))}\right| > \epsilon\right) \\
&\xrightarrow{P} 0,
\end{aligned}$$

where the final line follows from Lemma 5. Furthermore, from Lemma 4 we have  $F^{BJ}(S_u^*) \xrightarrow{a.s.} F^{NA}(S_u^*)$  under  $H_0$ , which implies that this result holds for  $F^{BJ}$ . Finally, by Lemma 3 all other score functions under consideration are maximizations over a monotonic transformation ( $T(F_{\alpha})$ ) of the continuous function  $F_{\alpha}^{NA}(S)$ ; therefore, the result for  $\max_{\alpha} F_{\alpha}^{NA}(S)$  will have a direct analogy for  $\max_{\alpha} T(F_{\alpha}^{NA}(S))$ .  $\square$

**Corollary 3.** Consider a sequence of critical values  $\max_{\alpha} \frac{M\phi(Z^t(\alpha))^2}{2(1-\Phi(Z^t(\alpha)))} + \epsilon_M$ , where  $\epsilon_M \rightarrow 0$  as  $Mn \rightarrow \infty$ . The above result would still hold, provided that  $h(M) = \max_{\alpha} \frac{M\phi(Z^t(\alpha))^2}{2(1-\Phi(Z^t(\alpha)))} (1 + o(1))$ .

Next, we analyze the score of the truly affected subset, when the null hypothesis is false.

**Lemma 6.** Under  $H_1(S^T)$ ,  $F^{NA}(S^T) \xrightarrow{a.s.} \max_{\alpha} (\beta(\alpha) - \alpha)^2 \frac{kMn}{2\alpha(1-\alpha)}$ .

*Proof.* First, recognize that  $N(S^T) \xrightarrow{P} kMn$  and recall that  $\mathbb{E}_{H_1(S^T)}[N_{\alpha}(S^T)] = N(S^T)\beta(\alpha)$ , from logic similar to Lemma 2. Therefore, we have the following:

$$\begin{aligned}
F^{NA}(S^T) &= \max_{\alpha} F_{\alpha}^{NA}(S^T) \\
&= \max_{\alpha} \frac{(N_{\alpha}(S^T) - N(S^T)\alpha)^2}{2N(S^T)\alpha(1-\alpha)} \\
&= \max_{\alpha} \frac{N(S^T) \left( \frac{N_{\alpha}(S^T)}{N(S^T)} - \alpha \right)^2}{2\alpha(1-\alpha)},
\end{aligned}$$

and

$$\frac{N_{\alpha}(S^T)}{N(S^T)} \xrightarrow{a.s.} \beta(\alpha).$$

Finally, by the continuous mapping theorem we have

$$F(S^T) \xrightarrow{a.s.} \max_{\alpha} (\beta(\alpha) - \alpha)^2 \frac{kMn}{2\alpha(1-\alpha)}.$$

$\square$

**Theorem 3.** Let  $n(x_t) \geq n \ \forall x_t \in D$ ,  $S^T$  be the truly affected subset of data, and  $k$  be the proportion of non-empty unique covariate profiles in the data (or cells in the tensor) that are affected under  $H_1(S^T)$ . Additionally, assume  $kMn \rightarrow \infty$ , then

$$P_{H_1} \left( \max_{S \in R} F(S) > h(M) \right) \rightarrow 1.$$

*Proof.* First, we note that under  $H_1(S^T)$

$$F(S^T) \leq F(S^*),$$

because the detected subset  $S^*$  is a maximization over all rectangular subsets (as defined in (8)) while  $S^T$  is one such subset. Now that we have a lower bound on  $F(S^*)$  under  $H_1(S^T)$ , we consider the critical value  $h(M) = \max_{\alpha} \frac{M\phi(Z^t(\alpha))^2}{2(1-\Phi(Z^t(\alpha)))} + \epsilon$ , for any  $\epsilon > 0$ , and the score function  $F^{NA}$ .

$$\begin{aligned} P_{H_1}(\text{Reject } H_0) &= P_{H_1}(F^{NA}(S^*) > h(M) + \epsilon) \\ &= P_{H_1} \left( F^{NA}(S^*) > \max_{\alpha} \frac{M\phi(Z^t(\alpha))^2}{2(1-\Phi(Z^t(\alpha)))} + \epsilon \right) \\ &\geq P_{H_1} \left( F^{NA}(S^T) > \max_{\alpha} \frac{M\phi(Z^t(\alpha))^2}{2(1-\Phi(Z^t(\alpha)))} + \epsilon \right) \\ &\rightarrow P_{H_1} \left( \max_{\alpha} (\beta(\alpha) - \alpha)^2 \frac{kMn}{2\alpha(1-\alpha)} > \max_{\alpha} \frac{M\phi(Z^t(\alpha))^2}{2(1-\Phi(Z^t(\alpha)))} + \epsilon \right) \quad (20) \\ &= P_{H_1} \left( \max_{\alpha} (\beta(\alpha) - \alpha)^2 \frac{kMn}{2\alpha(1-\alpha)} > \frac{M\phi(Z^t(\alpha_u^*))^2}{2(1-\Phi(Z^t(\alpha_u^*)))} + \epsilon \right) \\ &\geq P_{H_1} \left( (\beta(\alpha_u^*) - \alpha_u^*)^2 \frac{kMn}{2\alpha_u^*(1-\alpha_u^*)} > \frac{M\phi(Z^t(\alpha_u^*))^2}{2(1-\Phi(Z^t(\alpha_u^*)))} + \epsilon \right) \\ &= P_{H_1} \left( (\beta(\alpha_u^*) - \alpha_u^*)^2 \frac{kn}{2\alpha_u^*(1-\alpha_u^*)} > o(1) \right) \\ &= P_{H_1}(O(kn) > O(1)) \\ &\rightarrow 1. \end{aligned}$$

where (20) follows from Lemma 6. Furthermore, from Lemma 4 we have  $F^{BJ}(S_u^*) \xrightarrow{a.s.} F^{NA}(S_u^*)$  under  $H_0$ , which implies that comparing  $F^{BJ}$  to the same critical value  $h(M)$  will also yield the above result. Finally, by Lemma 3 all other score functions under consideration are maximizations over a monotonic transformation ( $T(F_{\alpha})$ ) of the continuous function  $F_{\alpha}^{NA}(S)$ ; therefore, the result for  $\max_{\alpha} F_{\alpha}^{NA}(S)$  will have a direct analogy for  $\max_{\alpha} T(F_{\alpha}^{NA}(S))$ .  $\square$

## Subset Correctness

We are still interested in studying the properties of our framework under  $H_1(S^T)$ , however here we are now concerned about the correctness of our detected subset  $S^*$ : as the objective is for the detected subset  $S^* = S^T$ . If  $s$  are data elements, i.e., the  $M$  non-empty cells in the tensor or unique covariate profiles in the data; the dataset  $D$  is the collection of these data elements, i.e.,  $D = \{s_1, \dots, s_M\}$ ; and that both  $S^*, S^T \subseteq D$ . The results in this section are general, and are therefore applicable to an unconstrained (or constrained)  $S^T$ ; therefore  $S^*$  will refer to the maximization over the unconstrained (or constrained) space in which  $S^T$  is defined.

We begin building our theory with a demonstration that the score functions can be re-written as additive functions if we condition on the value of the alternative hypothesis parameter  $\beta$ .

**Lemma 7.** For a given value of  $\beta \in (0, 1)$ ,  $F_\alpha^{NA}(S)$  and  $F_\alpha^{BJ}(S)$  are additive functions.

*Proof.* First we note that from the derivations of  $F_\alpha^{NA}(S)$  and  $F_\alpha^{BJ}(S)$ , that if we do not set  $\beta = \beta_{\text{mle}}(S)$  but instead treat  $\beta \in (0, 1)$  as a given quantity, then

$$\begin{aligned} F_{\alpha,\beta}^{NA}(S) &= \frac{N_\alpha(S)(\beta - \alpha)}{\alpha(1 - \alpha)} + \frac{N(S)(\alpha^2 - \beta^2)}{2\alpha(1 - \alpha)} \\ &= \frac{(\beta - \alpha)}{\alpha(1 - \alpha)} \left( \sum_{s_i \in S} n_\alpha(s_i) \right) + \frac{(\alpha^2 - \beta^2)}{2\alpha(1 - \alpha)} \left( \sum_{s_i \in S} n(s_i) \right) \\ &= \sum_{s_i \in S} \frac{(\beta - \alpha)}{\alpha(1 - \alpha)} n_\alpha(s_i) + \frac{(\alpha^2 - \beta^2)}{2\alpha(1 - \alpha)} n(s_i) \\ &= \sum_{s_i \in S} C_{\alpha,\beta}^{NA_1} n_\alpha(s_i) + C_{\alpha,\beta}^{NA_2} n(s_i) \\ &= \sum_{s_i \in S} \omega^{NA}(\alpha, \beta, n_\alpha(s_i), n(s_i)) \end{aligned}$$

and

$$\begin{aligned} F_{\alpha,\beta}^{BJ}(S) &= N_\alpha(S) \log \left( \frac{\beta}{\alpha} \right) + (N(S) - N_\alpha(S)) \log \left( \frac{1 - \beta}{1 - \alpha} \right) \\ &= N_\alpha(S) \log \left( \frac{\beta}{\alpha} \right) - N_\alpha(S) \log \left( \frac{1 - \beta}{1 - \alpha} \right) + N(S) \log \left( \frac{1 - \beta}{1 - \alpha} \right) \\ &= N_\alpha(S) \log \left( \frac{\beta(1 - \alpha)}{\alpha(1 - \beta)} \right) + N(S) \log \left( \frac{1 - \beta}{1 - \alpha} \right) \\ &= \log \left( \frac{\beta(1 - \alpha)}{\alpha(1 - \beta)} \right) \left( \sum_{s_i \in S} n_\alpha(s_i) \right) + \log \left( \frac{1 - \beta}{1 - \alpha} \right) \left( \sum_{s_i \in S} n(s_i) \right) \\ &= \sum_{s_i \in S} \left( \frac{\beta(1 - \alpha)}{\alpha(1 - \beta)} \right) n_\alpha(s_i) + \log \left( \frac{1 - \beta}{1 - \alpha} \right) n(s_i) \\ &= \sum_{s_i \in S} C_{\alpha,\beta}^{BJ_1} n_\alpha(s_i) + C_{\alpha,\beta}^{BJ_2} n(s_i) \\ &= \sum_{s_i \in S} \omega^{BJ}(\alpha, \beta, n_\alpha(s_i), n(s_i)) \end{aligned}$$

where all the  $C_{\alpha,\beta}$ 's are constants with respect to given values of  $\alpha, \beta$ .  $\square$

We now have that the score of a subset  $S$  can be decomposed into the sum of contributions (measured by a function  $\omega$ ) from each individual element contained within the subset. Next, we seek to demonstrate some important properties of the  $\omega$  functions. More specifically,  $\omega$  is a concave function with respect to  $\beta$ , which has two roots and a unique maximum.

**Lemma 8.**  $\omega^{NA}(\alpha, \beta, n_\alpha(s), n(s))$  is concave with respect to  $\beta$ , maximized at  $\beta_{\text{mle}}(s) = \frac{n_\alpha(s)}{n(s)}$ , and has two roots.

*Proof.* Firstly,

$$\begin{aligned} \frac{\partial \omega^{NA}(\alpha, \beta, n_\alpha(s), n(s))}{\partial \beta} &= \frac{n_\alpha(s) - n(s)\beta}{\alpha(1-\alpha)} \\ &= -\frac{n(s)}{\alpha(1-\alpha)}\beta + \frac{n_\alpha(s)}{\alpha(1-\alpha)} \end{aligned} \tag{21}$$

$$\begin{aligned} 0 \text{ (set)} &= -\frac{n(s)}{\alpha(1-\alpha)}\beta + \frac{n_\alpha(s)}{\alpha(1-\alpha)} \\ 0 &= -n(s)\beta + n_\alpha(s) \\ \beta &= \frac{n_\alpha(s)}{n(s)}, \end{aligned} \tag{22}$$

(21) shows that the first derivative is the equation of a line, with a negative slope, and (22) shows that this line has one root at  $\frac{n_\alpha(s)}{n(s)}$ . This implies  $\omega^{NA}$  is concave with respect to  $\beta$  (with at most two roots which we will refer to as  $\beta_{\min}(s)$  and  $\beta_{\max}(s)$ ) and is maximized at  $\frac{n_\alpha(s)}{n(s)}$ .  $\square$

**Lemma 9.**  $\omega^{BJ}(\alpha, \beta, n_\alpha(s), n(s))$  is concave with respect to  $\beta$ , maximized at  $\beta_{mle}(s) = \frac{n_\alpha(s)}{n(s)}$ , and has two roots.

*Proof.*

$$\begin{aligned} \frac{\partial \omega^{BJ}(\alpha, \beta, n_\alpha(s), n(s))}{\partial \beta} &= \frac{n_\alpha(s) - n(s)\beta}{\beta(1-\beta)} \\ 0 \text{ (set)} &= \frac{n_\alpha(s) - n(s)\beta}{\beta(1-\beta)} \\ 0 &= n_\alpha(s) - n(s)\beta + n_\alpha(s) \\ \beta &= \frac{n_\alpha(s)}{n(s)} \end{aligned}$$

shows that  $\omega^{BJ}$  is maximized (if it is concave) at  $\frac{n_\alpha(s)}{n(s)}$  and has at most two roots (which we will refer to as  $\beta_{\min}(s)$  and  $\beta_{\max}(s)$ ). Additionally,

$$\begin{aligned} \frac{\partial^2 \omega^{BJ}(\alpha, \beta, n_\alpha(s), n(s))}{\partial^2 \beta} \bigg|_{\beta=\frac{n_\alpha(s)}{n(s)}} &= -\frac{\beta^2 n(s) + (1-2\beta)n_\alpha(s)}{(\beta-1)^2 \beta^2} \bigg|_{\beta=\frac{n_\alpha(s)}{n(s)}} \\ &< 0 \end{aligned}$$

shows that  $\omega^{BJ}$  is concave with respect to  $\beta$ .  $\square$

Now that we have demonstrated that  $\omega$ , is concave, we now demonstrate a key insight about the difference between  $\alpha$  and  $\beta_{\max}(s)$  (i.e.,  $r_{\max}$ ) relative to the difference between  $\alpha$  and  $\beta_{mle}(s)$  (i.e.,  $r_{mle}$ ).

**Lemma 10.** With respect to  $\omega^{NA}(\alpha, \beta, n_\alpha(s), n(s))$ ,  $\frac{r_{\max}(s)}{r_{mle}(s)} = 2$ .

*Proof.* First, by Lemma 8, we know that, with respect to  $\beta$ ,  $\omega^{NA}$  is concave and has at most 2 roots

$(\{\beta_{\min}(s), \beta_{\max}(s)\})$ . Therefore, we have the following:

$$\begin{aligned}\omega^{NA}(\alpha, \beta, n_\alpha(s), n(s)) &= \frac{n_\alpha(s)(\beta - \alpha)}{\alpha(1 - \alpha)} + \frac{n(s)(\alpha^2 - \beta^2)}{2\alpha(1 - \alpha)} \\ 0 \text{ (set)} &= \frac{n_\alpha(s)(\beta - \alpha)}{\alpha(1 - \alpha)} + \frac{n(s)(\alpha^2 - \beta^2)}{2\alpha(1 - \alpha)} \\ &= 2n_\alpha(s)(\beta - \alpha) + n(s)(\beta^2 - \alpha^2) \\ &= (-n(s))\beta^2 + (2n_\alpha(s))\beta + (-2\alpha n_\alpha(s) + n(s)\alpha^2)\end{aligned}$$

$$\begin{aligned}\{\beta_{\min}(s), \beta_{\max}(s)\} &= \frac{-2n_\alpha(s) \pm \sqrt{(-2n_\alpha(s)) - 4(-n(s))(-2n_\alpha(s)\alpha + (n(s)\alpha)^2)}}{-2n(s)} \\ &= \frac{n_\alpha(s) \pm \sqrt{n_\alpha(s)^2 - 2n_\alpha(s)n(s)\alpha + (n(s)\alpha)^2}}{n(s)} \\ &= \frac{n_\alpha(s) \pm \sqrt{(n_\alpha(s) - 2N(S)\alpha)^2}}{n(s)} \\ &= \frac{n_\alpha(s) \pm (n_\alpha(s) - 2n(s)\alpha)}{n(s)} \\ &= \{\alpha, 2\beta_{\text{mle}}(s) - \alpha\}.\end{aligned}$$

This implies that  $\beta_{\max}(s) - \alpha = 2(\beta_{\text{mle}}(s) - \alpha)$  and  $r_{\max}(s) = 2r_{\text{mle}}(s)$ , with respect to  $\omega^{NA}$ .  $\square$

**Lemma 11.** *With respect to  $\omega^{BJ}(\alpha, \beta, n_\alpha(s), n(s))$ ,*

$$\frac{r_{\max}(s)}{r_{\text{mle}}(s)} \begin{cases} < 2 & \text{if } \beta_{\text{mle}}(s) > \frac{1}{2} \\ = 2 & \text{if } \beta_{\text{mle}}(s) = \frac{1}{2} \\ > 2 & \text{otherwise.} \end{cases}$$

*Proof.* First, by Lemma 9, we know that, with respect to  $\beta$ ,  $\omega^{BJ}$  is concave and has at most 2 roots  $(\{\beta_{\min}(s), \beta_{\max}(s)\})$ . One of the solutions of  $\omega^{BJ}$  must be  $\alpha$ , so let us assume that  $\beta_{\min}(s) = \alpha$ ; this will be true when  $\beta > \alpha$ , which intuitively corresponds to our case of interest: when the data elements contains more significant (extreme)  $p$ -values than expected. Furthermore, we know that  $\omega^{BJ}$  achieves a maximum at  $\beta_{\text{mle}} = \frac{n_\alpha(s)}{n(s)}$ . With these properties we can show our first case ( $1 \leq \frac{r_{\max}(s)}{r_{\text{mle}}(s)} < 2$ ) by first recognizing that trivially  $\beta_{\text{mle}} \leq \beta_{\max}$ , and  $\beta_{\text{mle}} - \alpha \leq \beta_{\max} - \alpha$ . To show the upper bound of our first case, it suffices to show that  $\omega^{BJ}(\alpha, \beta_{\text{mle}} - \epsilon, n_\alpha(s), n(s)) \geq \omega^{BJ}(\alpha, \beta_{\text{mle}} + \epsilon, n_\alpha(s), n(s))$  for some  $\epsilon > 0$ . Essentially, we are showing that the concave function  $\omega^{BJ}$  increases at a slower rate (until it reaches its maximum) than it decreases. This further implies that the distance between  $\beta_{\text{mle}}$  and  $\alpha$  is higher than  $\beta_{\max}$  and  $\beta_{\text{mle}}$  and therefore our desired result.

Recall from Lemma 9 that

$$\begin{aligned}\frac{\partial \omega^{BJ}(\alpha, \beta, n_\alpha(s), n(s))}{\partial \beta} &= \frac{n_\alpha(s) - n(s)\beta}{\beta(1 - \beta)} \\ &= n(s) \left[ \frac{\beta_{\text{mle}}(s) - \beta}{\beta(1 - \beta)} \right],\end{aligned}$$

which means the slope of  $\omega^{BJ}$  is proportional to  $\frac{\beta_{\text{mle}}(s) - \beta}{\beta(1 - \beta)}$ . We now compare the slope of around the inflection point  $\beta_{\text{mle}}(s)$ , and recognize that at

$\beta = \beta_{\text{mle}}(s) + \epsilon$  the slope is negative and its absolute value is proportional to  $\frac{\epsilon}{(\beta_{\text{mle}}(s) + \epsilon)(1 - \beta_{\text{mle}}(s) - \epsilon)}$

$\beta = \beta_{\text{mle}}(s) - \epsilon$  the slope is positive and its absolute value is proportional to  $\frac{\epsilon}{(\beta_{\text{mle}}(s) - \epsilon)(1 - \beta_{\text{mle}}(s) + \epsilon)}$ . Therefore,

$$\begin{aligned} \beta_{\text{mle}}(s) > \frac{1}{2} &\iff (\beta_{\text{mle}}(s) + \epsilon)(1 - \beta_{\text{mle}}(s) - \epsilon) < (\beta_{\text{mle}}(s) - \epsilon)(1 - \beta_{\text{mle}}(s) + \epsilon) \\ &\iff \frac{\epsilon}{(\beta_{\text{mle}}(s) + \epsilon)(1 - \beta_{\text{mle}}(s) - \epsilon)} > \frac{\epsilon}{(\beta_{\text{mle}}(s) - \epsilon)(1 - \beta_{\text{mle}}(s) + \epsilon)} \\ &\iff \frac{r_{\text{max}}(s)}{r_{\text{mle}}(s)} < 2. \end{aligned}$$

The demonstration of the remaining two conditions follow the precise same approach above, mutatis mutandis.  $\square$

Now that we have built up the necessary properties of the  $\omega$  functions, we now will discuss the sufficient conditions for the detected subset to be exactly correct  $S^* = S^T$ . To begin we introduce some additional notation

$$\begin{aligned} r_{\text{mle}-h}^{\text{aff}} &= \max_{s_i \in S^T} r_{\text{mle}}(s_i), \\ r_{\text{mle}-l}^{\text{aff}} &= \min_{s_i \in S^T} r_{\text{mle}}(s_i), \\ r_{\text{mle}-h}^{\text{unaff}} &= \max_{s_i \notin S^T} r_{\text{mle}}(s_i), \\ \eta &= \left( \frac{\sum_{s_i \in S^T} n(s_i) \alpha}{\sum_{s_i} n(s_i) \alpha} \right), \\ \nu - \text{homogeneous} &: \frac{r_{\text{mle}-h}^{\text{aff}}}{r_{\text{mle}-l}^{\text{aff}}} < \nu, \\ \delta - \text{strong} &: \frac{r_{\text{mle}-l}^{\text{aff}}}{r_{\text{mle}-h}^{\text{unaff}}} > \delta, \\ R &: (0, 1) \mapsto (0, 1). \end{aligned}$$

More specifically,  $R$  is an invertible function such that  $R: r_{\text{max}}(s) \mapsto r_{\text{mle}}(s)$ —i.e., if  $R$  is applied to  $r_{\text{max}}(s)$  it would produce the corresponding  $r_{\text{mle}}(s)$ . From Lemma 10 we know that with respect to  $\omega^{NA}$ ,  $R^{NA}(r) = \frac{r}{2}$ , while from Lemma 11 we know that with respect to  $\omega^{BJ}$ ,  $R^{BJ}(r) \leq \frac{r}{2}$  under certain conditions.

The first result we provide is a sufficient condition for guaranteeing that the detected subset includes all the elements from the true subset ( $S^* \supseteq S^T$ ). More specifically, we show that such a condition is sufficient homogeneity of the affected data elements: for a given value  $\nu$ , and any pair of the affected data elements ( $s_i, s_j \in S^T$ ), the anomalous signal observed in  $s_i$  is no more than  $\nu$ -times that which is observed in  $s_j$ .

**Theorem 4.** *Under  $H_1(S^T)$ , where  $S^T$  is a  $t$ -element subset of data elements that are not drawn from the null data generating process,  $\exists \nu > 1$  such that if the alternative process produces an observed signal in these elements that is  $\nu$ -homogenous, and at least 1-strong, then the highest scoring subset  $S^* \supseteq S^T$ .*

*Proof.* First, let  $\{s_{(1)}, \dots, s_{(t)}\}$  be the data elements in  $S^T$  sorted by the priority function (Theorem 1)  $G(s) = \frac{n_\alpha(s)}{n(s)} = \beta_{\text{mle}}(s)$ . By the assumption of an observed signal that is at least 1-strong, these data

elements are the  $t$  highest priority data elements. Additionally, let  $\nu = \frac{r_{\text{mle}-h}^{\text{aff}}}{R(r_{\text{mle}-h}^{\text{aff}})}$ . Therefore,

$$\begin{aligned}
\nu - \text{homogeneous} &\implies \nu > \frac{r_{\text{mle}-h}^{\text{aff}}}{r_{\text{mle}-l}^{\text{aff}}} \\
\therefore &\quad \frac{r_{\text{mle}-h}^{\text{aff}}}{R(r_{\text{mle}-h}^{\text{aff}})} > \frac{r_{\text{mle}-h}^{\text{aff}}}{r_{\text{mle}-l}^{\text{aff}}} \\
&\implies r_{\text{mle}-l}^{\text{aff}} > R(r_{\text{mle}-h}^{\text{aff}}) \\
&\implies R^{-1}(r_{\text{mle}-l}^{\text{aff}}) > r_{\text{mle}-h}^{\text{aff}} \\
&\implies \beta_{\text{max}}(s_{(t)}) - \alpha > \beta_{\text{mle}}(s_{(1)}) - \alpha \\
&\implies \beta_{\text{max}}(s_{(t)}) > \beta_{\text{mle}}(s_{(k)}) \quad (\forall k) \\
&\implies \beta_{\text{max}}(s_{(t)}) > \beta_{\text{mle}}(S^*) \\
\therefore &\quad \omega(\alpha, \beta_{\text{mle}}(S^*), n_\alpha(s_{(t)}), n(s_{(t)})) > 0 \\
\therefore &\quad |S^*| \geq t \\
\therefore &\quad S^* \supseteq S^T.
\end{aligned}$$

Intuitively,  $\beta_{\text{mle}}(s_{(t)})$  and  $\beta_{\text{mle}}(s_{(1)})$  are the respective smallest and largest  $\beta_{\text{mle}}$  of all the  $s \in S^T$ . Furthermore,  $\beta_{\text{mle}}(s_{(t)}) \leq \beta_{\text{mle}}(s_{(k)}) \leq \beta_{\text{max}}(s_{(t)})$   $k \in [1, t]$ , which means  $\beta_{\text{mle}}(S^*) \leq \beta_{\text{max}}(s_{(t)})$  for the optimal subset  $S^*$ . Moreover, the  $S^*$  that maximizes  $F_{\alpha, \beta}$  will include any data element  $s$  that would make a positive contribution to the score  $F_{\alpha, \beta}$  at the given value of  $\beta$  and  $\alpha$ . Such a positive contribution occurs when the concave  $\omega$  function of  $s$  is positive. At the optimal  $\alpha$  and  $\beta = \beta_{\text{mle}}(S^*)$  the  $\omega$  function for each of the  $\{s_{(1)}, \dots, s_{(t)}\}$  is positive because  $\beta_{\text{max}}$  (the larger root of the  $\omega$  functions) for each of these elements is greater than  $\beta_{\text{mle}}(S^*)$ .  $\square$

**Corollary 4.** *From Lemma 10 we know that with respect to  $\omega^{NA}$ ,  $\frac{r}{R(r)} = 2$ . Additionally, from Lemma 11 we know that with respect to  $\omega^{BJ}$ ,  $\frac{r}{R(r)} \leq 2$  under certain conditions. Therefore, we can conclude that 2-homogeneity (and 1-strength) is sufficient for  $S^* \supseteq S^T$  where with respect to  $F^{NA}$ ; to  $F^{BJ}$ , under some conditions; and to the other score functions described above, by Lemma 3. Essentially, if the observed proportion of p-values significant at  $\alpha^*$  across all of the  $s_i \in S^T$  are no more than two times larger than each other, the detected subset will include all the affected data elements.*

The next result we provide is a sufficient condition for guaranteeing that the detected subset will only include elements from the true subset ( $S^* \subseteq S^T$ ). More specifically, we show that such a condition is sufficient strength of the affected data elements; or intuitively, for a given value  $\delta$ , the anomalous signals observed in every affected data elements is at least more than  $\delta$ -times that of the unaffected data elements.

**Theorem 5.** *Under  $H_1(S^T)$ , where  $S^T$  is a  $t$ -element subset of data elements that are not drawn from the null data generating process,  $\exists \delta > 1$  such that if the alternative process produces an observed signal in these elements that is  $\frac{\delta}{\eta}$  - strong, then the highest scoring subset  $S^* \subseteq S^T$ .*

*Proof.* First, let  $D = \{s_{(1)}, \dots, s_{(t)}, s_{(t+1)}, \dots, s_{(M)}\}$  be the data elements sorted by the priority function (Theorem 1)  $G(s) = \frac{n_\alpha(s)}{n(s)} = \beta_{\text{mle}}(s)$ . By the assumption of  $\delta > 1$  (an observed signal that is at least

1-strong),  $S^T = \{s_{(1)}, \dots, s_{(t)}\}$ . Additionally, let  $\delta = \frac{R^{-1}(r_{\text{mle}-h}^{\text{unaff}})}{r_{\text{mle}-h}^{\text{unaff}}}$ . Therefore,

$$\begin{aligned}
\delta - \text{strong} &\implies \delta < \frac{r_{\text{mle}-l}^{\text{aff}}}{r_{\text{mle}-h}^{\text{unaff}}} \\
\therefore &\quad \frac{R^{-1}(r_{\text{mle}-h}^{\text{unaff}})}{\eta r_{\text{mle}-h}^{\text{unaff}}} < \frac{r_{\text{mle}-l}^{\text{aff}}}{r_{\text{mle}-h}^{\text{unaff}}} \\
\implies &\quad R^{-1}(r_{\text{mle}-h}^{\text{unaff}}) < \left( \frac{\sum_{s_i \in S^T} n(s_i) \alpha}{\sum_{s_i} n(s_i) \alpha} \right) r_{\text{mle}-l}^{\text{aff}} \\
&= \frac{\sum_{s_i \in S^T} r_{\text{mle}-l}^{\text{aff}} n(s_i)}{\sum_{s_i} n(s_i)} \\
&\leq \frac{\sum_{s_i \in S^T} r_{\text{mle}}(s_i) n(s_i)}{\sum_{s_i} n(s_i)} \quad (\text{b/c } r_{\text{mle}}(s_i) \geq r_{\text{mle}-l}^{\text{aff}} \quad \forall s_i \in S^T) \\
&\leq \frac{\sum_{s_i \in S^T} r_{\text{mle}}(s_i) n(s_i) + \sum_{s_i \notin S^T} r_{\text{mle}}(s_i) n(s_i)}{\sum_{s_i} n(s_i)} \\
&= \frac{\sum_{s_i} r_{\text{mle}}(s_i) n(s_i)}{\sum_{s_i} n(s_i)} \\
&= \frac{\sum_{s_i} \left( \frac{n_{\alpha}(s_i)}{n(s_i)} - \alpha \right) n(s_i)}{\sum_{s_i} n(s_i)} \\
&= \frac{\sum_{s_i} n_{\alpha}(s_i) - n(s_i) \alpha}{\sum_{s_i} n(s_i)} \\
&= \frac{\sum_{s_i} n_{\alpha}(s_i) - \sum_{s_i} n(s_i) \alpha}{\sum_{s_i} n(s_i)} \\
&= \frac{\sum_{s_i} n_{\alpha}(s_i)}{\sum_{s_i} n(s_i)} - \alpha \\
\therefore &\quad \beta_{\text{max}}(s_{(t+1)}) - \alpha < \beta_{\text{mle}}(D) - \alpha \\
\implies &\quad \beta_{\text{max}}(s_{(t+1)}) < \beta_{\text{mle}}(s_{(t)}) \\
\implies &\quad \beta_{\text{max}}(s_{(t+1)}) < \beta_{\text{mle}}(S^*) \\
\therefore &\quad \omega(\alpha, \beta_{\text{mle}}(S^*), n_{\alpha}(s_{(t+1)}), n(s_{(t+1)})) < 0 \\
\implies &\quad |S^*| \leq t \\
\therefore &\quad S^* \subseteq S^T
\end{aligned}$$

Intuitively,  $\beta_{\text{mle}}(s_{(t)})$  and  $\beta_{\text{mle}}(s_{(t+1)})$  are the respective smallest affected and largest unaffected  $\beta_{\text{mle}}$  values. Furthermore,  $\beta_{\text{max}}(s_{(t+1)}) \leq \beta_{\text{mle}}(s_{(t)})$ , which means  $\beta_{\text{max}}(s_{(t+1)}) \leq \beta_{\text{mle}}(S^*)$  for the optimal subset  $S^*$ . Moreover, the  $S^*$  that maximizes  $F_{\alpha, \beta}$  will not include any data element  $s$  that makes a non-positive contribution to the score  $F_{\alpha, \beta}$  at the given value of  $\beta$  and  $\alpha$ . Such a non-positive contribution occurs when the concave  $\omega$  function of  $s$  is non-positive. At the optimal  $\alpha$  and  $\beta = \beta_{\text{mle}}(S^*)$  the  $\omega$  function for each of the  $\{s_{(t+1)}, \dots, s_{(M)}\}$  are non-positive because  $\beta_{\text{max}}$  (the larger root of the  $\omega$  functions) for each of these elements is less than  $\beta_{\text{mle}}(S^*)$ .  $\square$

**Corollary 5.** *From Lemma 10 we know that with respect to  $\omega^{NA}$ ,  $\frac{R^{-1}(r)}{r} = 2$ . Additionally, from Lemma 11 we know that with respect to  $\omega^{BJ}$ ,  $\frac{R^{-1}(r)}{r} \geq 2$  under certain conditions. Therefore, we can conclude that 2-strength is sufficient for  $S^* \supseteq S^T$  where with respect to  $F^{NA}$ ; to  $F^{BJ}$ , under some conditions; and to the other score functions described above, by Lemma 3. Essentially, if the observed proportion of p-values significant at  $\alpha^*$  across all of the  $s_i \in S^T$  are at least two times larger than the  $s_i \notin S^T$ , then the detected subset will only include the affected data elements.*

**Theorem 6.** Under  $H_1(S^T)$ , where  $S^T$  is a  $t$ -element subset of data elements that are not drawn from the null data generating process, if the alternative process produces an observed signal that is  $\nu$  – homogenous and  $\frac{\delta}{\eta}$  – strong, then  $S^* = S^T$ .

*Proof.*

$$\begin{aligned}
 & \because \nu - \text{homogenous} \implies S^* \supseteq S^T \quad (\text{by Theorem 4}) \\
 & \because \frac{\delta}{\eta} - \text{strong} \implies S^* \subseteq S^T \quad (\text{by Theorem 5}) \\
 & \therefore \quad \quad \quad S^* = S^T
 \end{aligned}$$

□